

AUTOMATIC WHITE BLOOD CELL DIFFERENTIAL
CLASSIFICATION

A THESIS IN MECHATRONICS

Presented to the faculty of the American University of Sharjah
School of Engineering
in partial fulfillment of
the requirements for the degree

Master of Sciences

by
JUMA A. BIN DARWISH AL-MUHAIRY
B.S. 2001

Sharjah, UAE

June, 2005

© 2005

JUMA A. BIN DARWISH AL-MUHAIRY

ALL RIGHTS RESERVED

AUTOMATIC WHITE BLOOD CELL DIFFERENTIAL CLASSIFICATION

Juma A. Bin Darwish Al-Muhairy, Candidate for the Master of Science Degree

American University of Sharjah, 2005

ABSTRACT

The characteristics (quantity, shape and color) of the white blood cell (WBC) can give vital information about a patient's health. Hematologists, with the aid of microscopes, use their experience to classify WBCs and make appropriate reporting and recommendations to physicians. Automating the segmentation and classification of WBC could provide a useful tool in medical diagnoses.

In this work, computer-based segmentation and classification of the four main classes of WBC (Neutrophils, Eosinophils, Lymphocytes, and Monocytes) were completed. Soft computing algorithms including neural network (NN) and polynomial classifiers (PC) were used for WBC classification, while watershed and thresholding based on size, shape, color and texture characteristics were used to segment WBC from Red Blood Cells RBC, platelets, cell fragments and stains. Furthermore, characteristics of the WBC were utilized in association with the intelligent systems to classify these WBC's to different classes. The number and distribution of different classes of WBC has medical indications (e.g. high Neutrophils count may possibly imply cancer, whereas high Lymphocytes count could lead to AIDS).

To classify WBC morphological based features, Discrete Cosine Transform (DCT) based features and Discrete Wavelets Transform (DWT) based features were used as input feature vectors to the Neural Networks NN and Polynomial Classifiers PC. Various

feature extraction modalities and classifiers were tested on blood data obtained from patients at Twam Hospital in UAE. Combining color morphological and DWT features in association with the PC second order classifier achieved a Classification Accuracy (CA) of 99.3%. Other advantages of using PC was that it needed less computational requirements and classification was independent on various user-set parameters as it was the case of NN. In addition, PC proven to be more reliable and consistent in terms of results compared to NN.

TABLE OF CONTENTS

ABSTRACT.....	iii
LIST OF FIGURES	vii
LIST OF Tables	ix
Acknowledgement	x
CHAPTER 1 BACKGROUND AND SIGNIFICANCE.....	1
1.1 The Problem.....	1
1.2 Literature Review.....	2
1.3 Methodology	10
CHAPTER 2 SEGMENTATION	12
2.1 Introduction.....	12
2.2 Proposed Segmentation Methodology	13
2.2.1 Image Gathering and Pre-Processing.....	14
2.2.2 Pre-Segmentation and Thresholding.....	15
2.2.3 Watershed Transformation and Region Properties	19
2.2.4 WBC Detection and Post-Segmentation.....	20
2.3 Results and Discussion.....	21
CHAPTER 3 FEATURE EXTRACTION.....	27
3.1 Introduction.....	27
3.2 Types of Features	29
3.2.1 Morphological Based Features	29
3.2.2 Discrete Wavelet Transform Based Features.....	37
3.2.3 Discrete Cosine Transform (DCT) Based Features	43
CHAPTER 4 CLASSIFICATION.....	48
4.1 Introduction.....	48
4.2 Classification Using Neural Network	48
4.3 Classification using Polynomial Classifier	51
CHAPTER 5 Results and Discussion of the Classification.....	54
5.1 Introduction.....	54
5.1.1 DWT Based Classification	56
5.1.2 DCT Based Classification	58
5.1.3 Morphological Based Classification.....	63

5.1.4	Combination of Morphological, DWT and DCT Features for Classification.....	68
CHAPTER 6	CONCLUSION AND FUTURE WORK.....	74
References.....		76

LIST OF FIGURES

Figure	page
Fig. 1.1 Blood composition [4]	3
Fig. 1.2 Location of the bone marrow in bones and types of blood cells produced (http://web1.tch.harvard.edu/cfapps/A2ZtopicDisplay.cfm?)	5
Fig. 1.3 Blood smear image	6
Fig. 2.1 Image acquiring, enhancement and segmentation flow chart (all concepts to be discussed further in the next sections)	13
Fig. 2.2 Original images as captured from microscope b) Enhanced image color	15
Fig. 2.3 a) Original image b) Image subtracted	16
Fig. 2.4 a) Original image b) Gray image	16
Fig. 2.5 a) Original image b) Hue image c) Saturation image d) Intensity image	17
Fig. 2.6 a) Original image b) Red image c) Green image d) Blue image	18
Fig. 2.7 Blood image after applying Otsu's adaptive	19
Fig. 2.8 Watershed output of the image shown in Fig.2.6b	20
Fig. 2.9 RGB (Red Channel) and HSI model space channels comparison	22
Fig. 2.10 Using the normal and the adaptive algorithm	22
Fig. 2.11 Comparison between segmented images	23
Fig. 2.12 Segmentation of Lymphocytes using the proposed method	25
Fig. 2.13 Good and inadequate segmentation of Eosinophils WBC	25
Fig. 3.1 Area of WBC	29
Fig. 3.2 Eccentricity (ECC)	30
Fig. 3.3 Number of objects (NOO)	31
Fig. 3.4 Percentage of Nucleus to Cytoplasm (PNC)	32
Fig. 3.5 a) Monocyte cell b) Lymphocyte cell	32
Fig. 3.6 Average Red intensity channel (Actual data and Average of the Actual data)	33

Fig. 3.7 Average Blue intensity channels (Actual data and Average of the Actual data)	34
Fig. 3.8 Average Green intensity channel (Actual data and Average of the Actual data)	34
Fig. 3.9 a) Image boxes b) Neutrophils image divided to four areas	35
Fig. 3.10 Average of pixels' in box 2 per Red channel of the RGB color model	36
Fig. 3.11 Red Channel of Nucleus Color Average (Actual data and Average of the Actual data)	37
Fig. 3.12 Wavelets Coefficient [26, 28]	38
Fig. 3.13 a) Wavelets Decompositions up to 3 resolution levels b) Lymphocyte decomposition c) Neutrophil decomposition	41
Fig. 3.14 DWT Image Structure Showing the Highlighting Diagonal and Energy coefficients	42
Fig. 3.15 Average of the diagonal coefficient using Haar Wavelets for the first resolution level (image is decomposed for 4 resolution levels)	43
Fig. 3.16 Horizontal DCT Matrices of Coefficients	44
Fig. 3.17 Averaging the horizontal information of the DCT coefficients row # 4 (Actual data and Averages of the Actual data)	45
Fig. 3.18 Block based grouping of DCT diagonal coefficients	46
Fig. 3.19 Sample DCT average for the red component (Actual data and Average of the Actual data)	47
Fig. 4.1 McCulloch-Pitts model of an artificial neuron (Basic Model of Neuron) [30]	49
Fig. 4.2 General Structure for feed forward NN [2,30]	50
Fig. 4.3 Learning Rules (Training Algorithms) Diagram [30]	51
Fig. 5.1 AI System Basic	54

LIST OF TABLES

Table	Page
Table 1.1 Differential staining morphology of different blood cell types [5, 6]	4
Table 2.1 Sample Segmentation of WBC from typical BC images	12
Table 2.1 Segmentation accuracy for various types of WBC	24
Table 3.1 WBC classes to be classified	28
Table 5.1 Desired AIs classifier outputs for WBC classification	55
Table 5.2 Comparison between classifiers outcomes using DWT Features based on Haar with 4 resolution levels	57
Table 5.3 DCT Data Sets of Horizontal Row Averaging	58
Table 5.4 Comparison between Features outcomes via (PC and NN) classifier using DCT Horizontal Row Averaging	59
Table 5.5 DCT Data Sets of Block Grouping	61
Table 5.6 Comparison between Block Features data sets as input to NN classifier	62
Table 5.7 Morphological Features modalities used per experiment	64
Table 5.8 Comparison between classifier and modalities features using PC based on morphological features	66
Table 5.9 Comparison between classifier and modalities features using NN based on morphological features	67
Table 5.10 Data Sets used for the combination of features	69
Table 5.11 Comparison between classifier and modalities features using PC (Bolded Numbers represents the highest Classification Accuracy)	71
Table 5.12 Comparison between classifiers and modalities features using NN	72

Acknowledgement

First, I would like to thank Allah for his support to start and finish this work. Second, I would like to express my appreciation to my supervisor Dr. Yousef Al-Assaf for his unlimited support and valuable guidance, who encouraged me to publish this work, which resulted in a paper accepted in the International Federation of Automatic Control, 16th World Congress Committee (IFAC 2006 Committee).

I would also like to mention those who provided me with the needed support to finish my thesis. Particular thanks go to Mr. Wessam Khiwi and Mrs. Maryam Al-Shamsi from the Hematologist Department at Twam Hospital in UAE. They had provided me with hundreds of medical images and given me lots of suggestions and ideas for new interesting problems in medical imaging.

Last but not least, I would like to thank my family and my friends for their love and never-ending support.

Juma A. Bin Darwish Al-Muhairy

CHAPTER 1

BACKGROUND AND SIGNIFICANCE

1.1 The Problem

The medical community has been established to take care of human health with knowledgeable and proficient people who are specialized in health science [1,2,3]. With the technological advances in medical field, the need for faster and more accurate analysis tools is essential (e.g. x-ray machines, complete blood count machines...etc). These automated medical tools are essential for diagnosing patients. They are necessary for supporting medical doctors in accurately providing future prognoses of the conditions and how to cure them [2, 3]. The positive side of utilizing the new technologies is that it lessens the risk of giving wrong diagnoses, providing much quicker diagnoses for patients' conditions, and reducing doubtful opinions of doctors [2,4].

With the increasing number of diseases today [1], there are many patients to look after and many more healthy people who require medical maintenance in order to maintain their good health. Therefore, a fast, durable, automated and intelligent system is required for doctors to carry out the necessary diagnoses [1,2,4].

Some of the main laboratories requirement are automated; and intelligent systems are used for bone marrow analysis and differential count of blood components (e.g. to count the number of red and white blood cells, platelets...etc). Any effort to help in reducing errors and speeding up the different types of blood diagnosis tools is valuable because it lessens the workload of the lab diagnosis experts [1-3,5,6]. WBC differential diagnosis is vital in today's medical industry because it helps in correctly analyzing the conditions of healthy and unhealthy patients. The normality and abnormality conditions of WBC provide hematologists with a great amount of useful data and knowledge about a patient's condition [5].

Since hematologists conduct blood tests, it is these experts who use the two most common types of analyzing tools for diagnosing and screening blood smears [1, 2]:

- Complete Blood Count (CBC)
- Differential Blood Count (DBC)

CBC machine counts the number of each type of blood composition using an instrument called a “Cytometer” which is useful in the blood lab for counting the blood cells and components for each sample taken from patients [1, 2]. The disadvantage of CBC is that it gives only general, not specific, information about blood composition. On the other hand, DBC is much more efficient and reliable in terms of giving the exact number of blood composition. Differential blood counting machines operate by sampling human blood and drawing a small amount of blood through narrow tubing. Inside this tubing there are sensors that count the number of each blood cell type, which are going through the tube (those sensors have the ability to identify the type of each blood cell). The drawbacks of this process are that the DBC sensors need occasional calibration, the maintenance cost is high, and the DBC might misclassify some cells (in which case an expert hematologist has to classify the cell). Usually examiners in the lab use the manual count as a way to confirm the DBC results. This manual process is done by the specialists who count one hundred WBC using blood film generated from each blood drop smear slide [1, 2]. They count the presence of each type of WBC and calculate the percentage of each class of WBC in the sample under examination. As a result, the hematologist and the doctor will have a lot of valuable information about the patient’s condition. However, the disadvantage of the manual count is that it is subject to human error and the count is based on a much smaller sample size. Manual counting has the advantage in that it can identify blood cells that may be misidentified by an automated counter and DBC.

It is apparent why an automated system can result in reducing workload and ensuring the calculation of blood composition done by hematologists.

1.2 Literature Review

Blood is a fluid in the human body that has the major task of transporting oxygen, salts, hormones, carbon dioxide and many other components from one place to another in order

to maintain a healthy life. Blood composition is made of a fluid called “plasma” and three additional types of cells as shown in Fig.1.1. The figure shows blood cells and their role in the human body:

- Red Blood Cell (RBC)
- White Blood Cell (WBC)
- Platelets cells

There are also some cell fragments, which exist in the human blood.

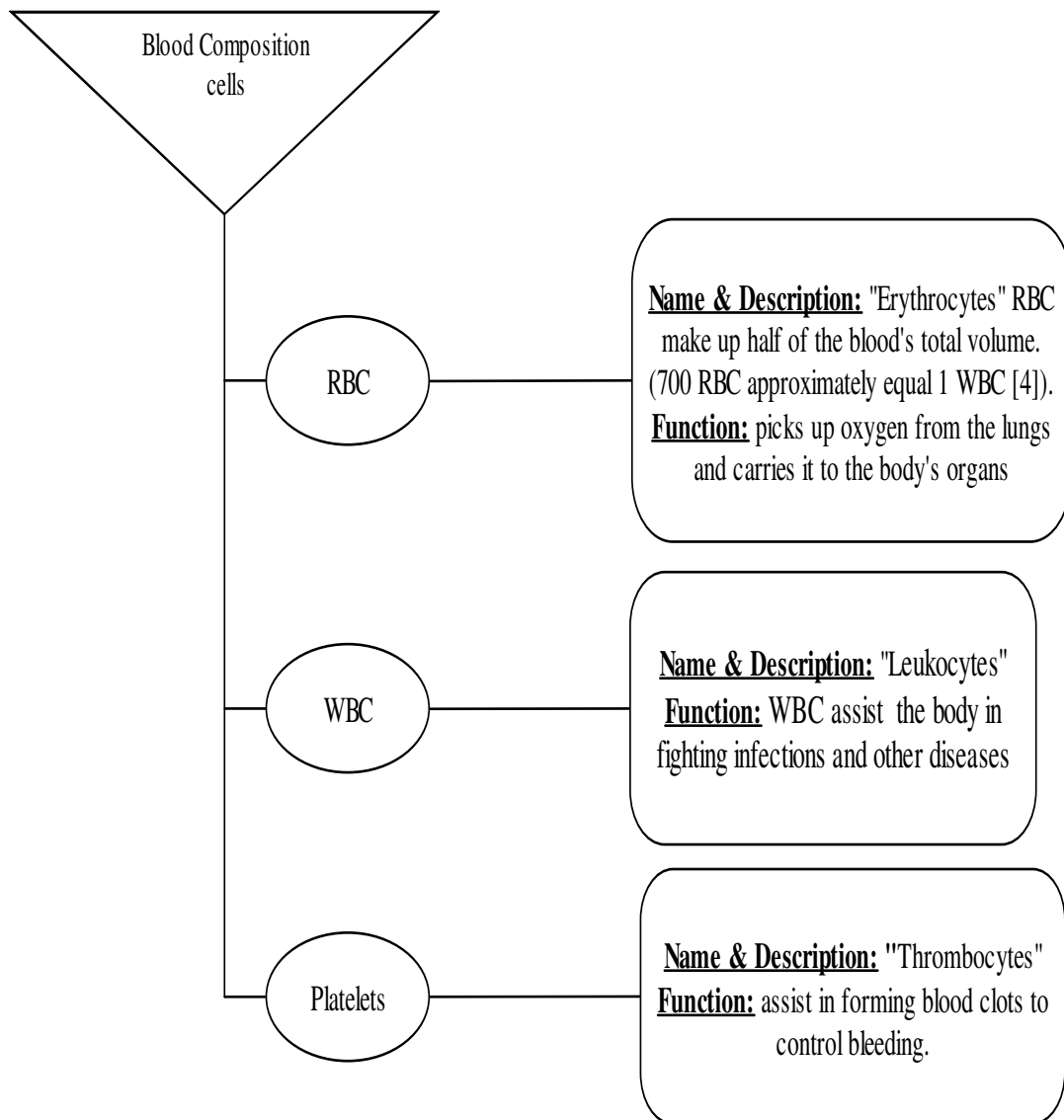


Fig. 1.1 Blood composition [4]

Blood Cells (BC) are formed inside the bones in the “bone marrow” [4]. The “Stem Cell” is considered as the origin of all BC. The differentiation process occurs when stem cells get mature. At the beginning, immature cells are called blasts, which then develop into mature BCs. As soon as BC is mature enough, it is released into the blood and circulated throughout the entire body to perform its individual functions.

Table 1.1 Differential staining morphology of different blood cell types [5, 6]

Cell Type	Cytoplasm	Nucleus	Granules	Central Granules
Red Blood Cell				
RBC	Orange to pink to rose			
WBC Types				
Lymphocytes	Light blue	Deep blue to violet		
Eosinophils			Orange to pink	
Monocytes	Pale gray to blue	Deep bluish to purple		
Neutrophils	Pale pink	Deep blue to violet	Purple to lilac	
Basophiles			Deep blue to violet	
Platelets				
Platelets				Red to purple surrounded by light blue

Blood Cells are classified according to their shape, color and texture, as shown in Table 1.1, which summarizes these differences between the cell composition.

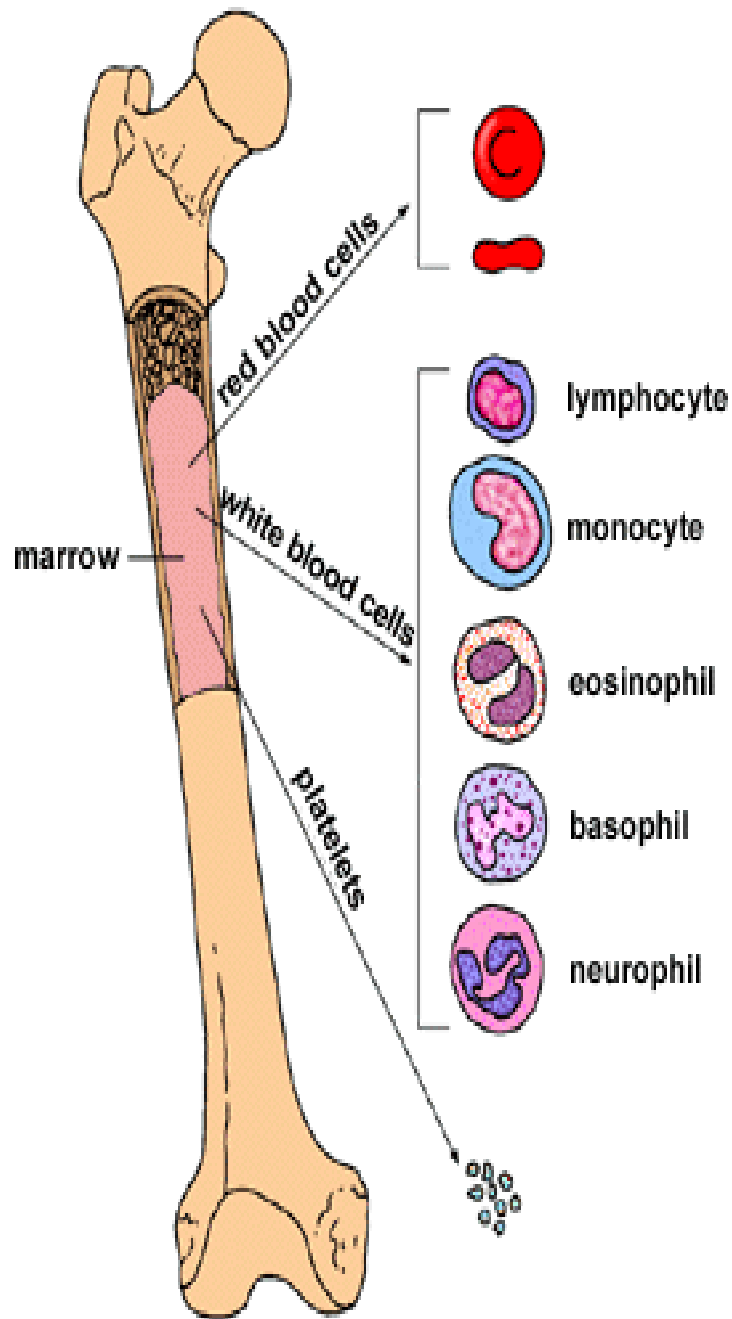
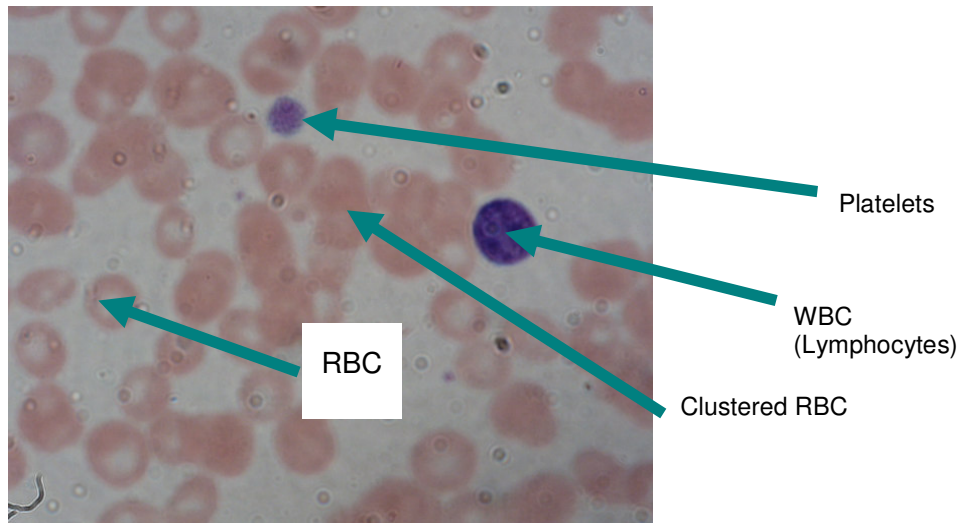
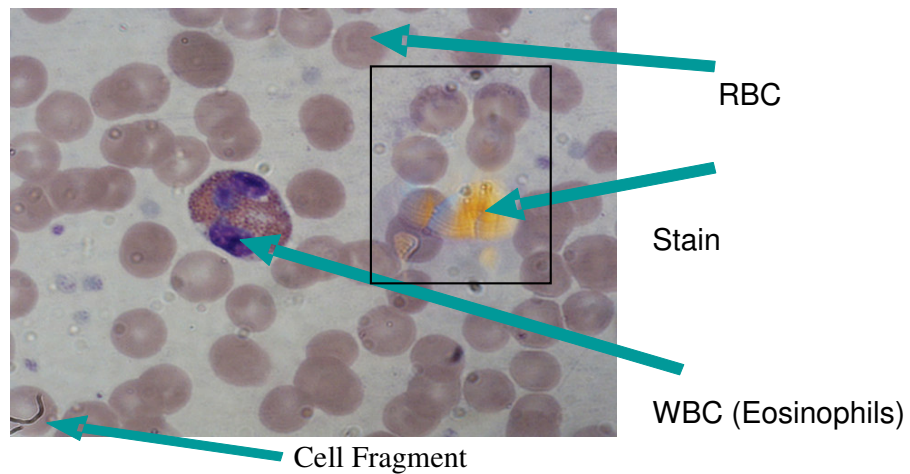


Fig. 1.2 Location of the bone marrow in bones and types of blood cells produced
 (<http://web1.tch.harvard.edu/cfapps/A2ZtopicDisplay.cfm?>)

Fig. 1.2 explains human bone marrow and the blood composition that are produced in human bone marrow.



a)



b)

Fig. 1.3 Blood smear image

Also, Fig 1.3 a and b show real blood smear composition. This is a sample image of a blood smear as seen by the medical microscope that demonstrates typical blood composition, including WBC, RBC, platelets and cell fragments.

WBC differentiation is important for early detection of diseases. For example, in case of a patient diagnosed with Leukemia (Blood Cancer), the body produces more amounts of immature or abnormal WBC to help the body defeat this disease through its immune system.

In order to conduct a proper diagnosis of Leukemia, the physician must take a sample of blood from the middle of the bone. The collected cells, bone marrow biopsy, and bone

sample and tissues, are screened under a microscope manually and a special analysis is conducted to detect the cancerous BC [5] (carcinogenic).

The need to automate this process helps reduce human errors in determining the cancerous cells or any other abnormalities of WBC. It will also help speed up the process and provides more efficient diagnosis tool for many other blood diseases (e.g. blood cancer, anemia, AIDS or bone marrow cancer).

In many of the recent research studies, more attention has been paid to automate the DBC for a fast diagnosis of blood cancer symptoms and many other diseases. Sysmex Europe GMBH Company conducted a research which resulted in a state of the art system DiffMaster which was based on image processing analysis application [7]. (DiffMaster) acquired the images through a high resolution camera which was mounted on microscope. The image processing techniques were applied to extract the needed feature (e.g. size, color, texture features...etc) to analyze different types of WBC [8]. The camera then took a snap shot of the sample, sent it to the computer in order to be examined and pre-classify the WBC using NN. The classification accuracy percentage is 89% [7].

In addition, the University of Kaiserslautern and the Westpfalz-Klinikum initiated research to automate the diagnosis process of WBC differentials [9]. Their system automatically analyzed the stained blood and bone marrow slides under the microscope. The main objective was to build a device that could count the different lineage and maturity levels of WBC [9] to determine the occurrence of leukemia and other diseases. Only segmentation of WBC is attempted in this research using image processing tool boxes in Matlab.

Sabino et al [10] calculated four textural features of WBC based on Gray Level Co-occurrence Matrices (GLCM) (energy, entropy, inertia and local homogeneity) for Lymphocytes. WBC cell differentiation test these features to recognize leukocyte cells. Their Experimental results demonstrated that texture parameters were vital to distinguish between the five types of normal leukocytes and chronic lymphocytic leukemia. The input to their automatic pattern recognition classifier was quantitative features generated from GLCM which proven useful and given 96% classification accuracy.

Zheng, Milthorpe and Johnes [11] attempted to classify manually cropped image data for WBC. They used intensity values as input to Neural Network NN. A classification

accuracy of 97% with three layers NN and 98% with four layers NN based on back propagation algorithm was achieved. In this paper, no reference was made to the number of images used and the condition of the cells as being healthy or diseased.

Yang, Foran and Meer had utilized and enhanced the algorithm of the Image Guided Decision Support Software (IGDS) to segment WBC. In their research, they investigated the design, development, and implementation of a “robust color Gradient Vector Flow (GVF) active contour model for performing segmentation” [12]. Their database consisted of 1,791 images of blood smear samples. They used the “Luv” color space (another color space transformed from RGB in which L component defines the luminance, and u, v define chrominance). Also, they develop a color gradient and robust least square estimation into the traditional GVF snake. Their segmentation results were comparable with the one obtained using traditional color GVF snake, mean-shift approach and several other commonly used segmentation strategies.

Sinha and Ramakrishnan [13] used color blood smear image of normal WBC in peripheral blood. They used HSI-equivalent of the image, K-Means clustering followed by EM-algorithm to segment WBC. Also, they segmented cytoplasm and nucleus from each other. Then, they extracted the features of the visual cues of shape, color and texture. A variety of classifiers were explored using different combinations of feature sets. For training the classifiers, a 50 patterns database was used with about 10 samples from each class (WBC has five classes). The test data, which was separated in advance from the training set, consisted of 34 patterns, fairly represented by each class. NN achieved classification accuracy of 97% (the highest), while Support Vector Machine (SVM) accomplished 94%.

Ongun et al. [14] used color smear images, containing both immature and peripheral WBC cells. Ongun applied morphological pre-processing combined with fuzzy patch labelling to segment WBC from other blood elements. From each WBC image they extracted the morphological features such as shape, color and texture features. Shape features are areas of cell and nucleus, ratio of nucleus to overall cell area, cell perimeter, compactness and boundary energy of the nucleus. Color histogram, mean and standard deviation of the color components in CIE-Lab domain represent the color features. Where the CIE-lab refers to an organization called “Commission Internationale de l'Eclairage”. CIE has determined standard values that are used to measure color. The

values used by CIE are called L^* (represents the difference between dark (where $L^*=0$) and light (where $L^*=100$), a^* (represents the difference between green and red), b^* (represents the difference between yellow and blue) and the color measurement approach is called CIE-lab. Texture features include contrast, homogeneity and entropy derived from the GLCM. The feature vector consisted of around 57-dimensional feature set used for classification with various classifiers. Using Support Vector Machine (SVM) a peak performance of 91% was achieved on a mixed set of 58 “lymphoproliferative” cases [14]. The condition of the cells as being healthy or diseased was, also, not mentioned.

Bikhet et al. [15] applied segmentation and classification of the five types of WBC’s presented in peripheral blood. They used Gray image of blood smears. The use of hierarchical thresholdings helps allocate and segment WBC. The ratio of nucleus to cell area, circularity measure average Gray level and area of nucleus and cytoplasm are used as features extracted from each WBC image. In their research, they achieved classification accuracy of 90% using 71 cells sample image. In their paper, there was no indication if the cells used are being healthy or diseased. Besides, the classifier used has not been disclosed.

Park [16] applied segmentation and classification on low resolution Gray Images of immature WBC. The feature vector set consisted of shape, texture and statistical color features. NN had resulted in a classification accuracy of 70%.

From the above literature, most of the research presented focused on NN as their main classifier; and NN produced adequate classification results. However, only Ongun applied SVM (which generated 94% classification accuracy) as new a contribution to classifying WBC. With regard to features used, morphological features including shape, texture and statistical color features were commonly used across the literature and gave reasonable differentiation. Yet, GLCM was used in several researches and alone manage to satisfactorily differentiate WBC classes. Limited number of researchers used different algorithm to segment WBC from original images. For example, fuzzy patch labelling was used to segment WBC. Nevertheless, there was no indication on the performance of their segmentation models adopted.

The contribution of this thesis covers the implementation of a segmentation algorithm. This algorithm mainly focuses on extracting the WBC presented on Blood image. Then,

a feature vector which consists of morphological features including geometrical, shape, texture and color is adopted in this contribution. In addition, the Discrete Cosine Transform (DCT) and Discrete Wavelet Transform (DWT) feature, also, to be included in the feature vector produced. Finally, neural network and polynomial classifiers are to be used and the performance of each will be compared with one another.

1.3 Methodology

This work is done in collaboration with Hematology Department at Twam Hospital which is mainly concerned with the diagnoses and treatment of cancer.

The proposed solution for WBC differentials is to implement an automated classifier system to determine classes of WBC [2-5, 9-16].

Fig. 1.4 shows block diagram of the process that was adopted in this work in order to automate the classification of WBC.

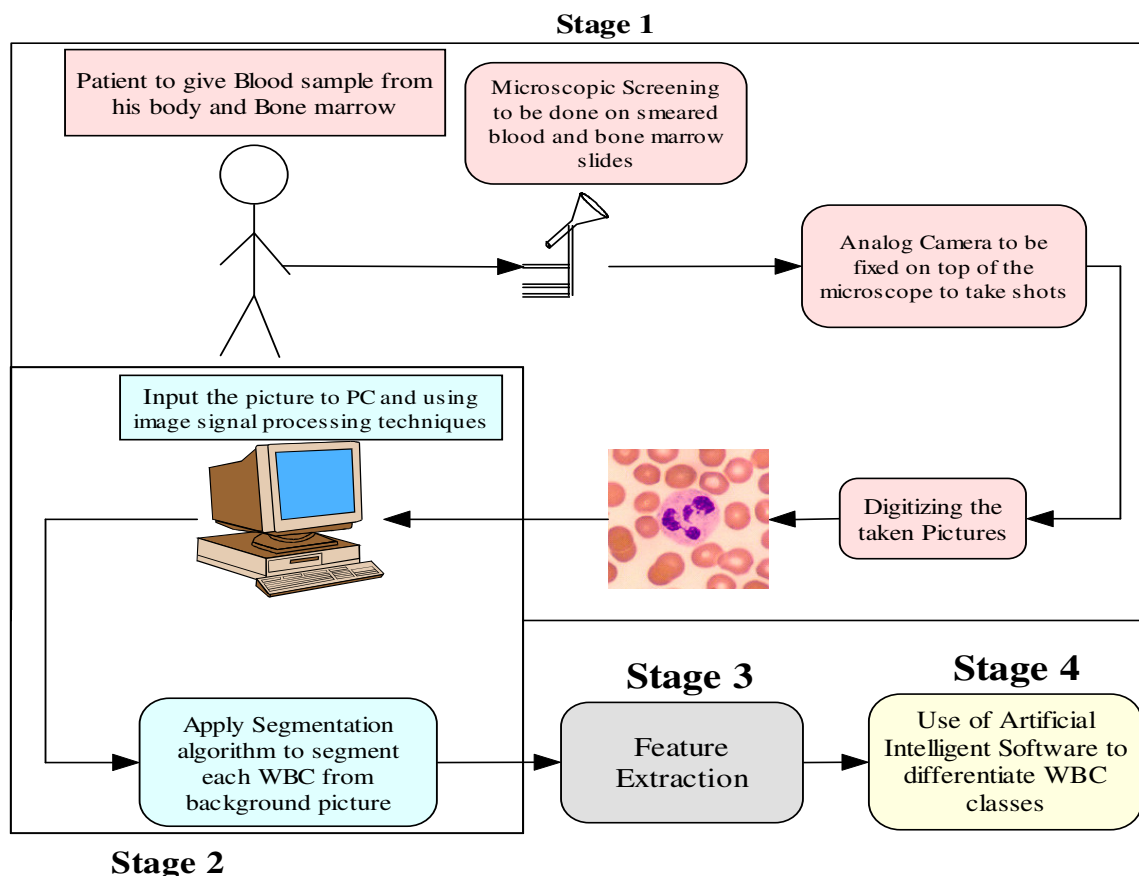


Fig. 1.4 Stages of WBC classification

The process consists of the following stages:

1. Gathering the blood samples and applying image processing techniques
2. WBC cell segmentation
3. Feature Extraction
4. WBC classification

Chapter two summarizes and describes some techniques developed for WBC segmentation. Chapter three discusses feature extraction methodologies and gives necessary parameters that will be used as main feature input vector. Chapter four discusses the importance of classification techniques involving Neural Networks NN and Polynomial Classifier PC. Chapter five summarizes the outcomes and suggests future plans.

CHAPTER 2

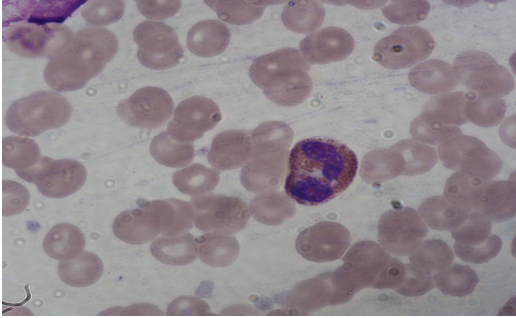
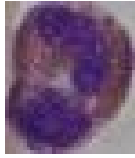
SEGMENTATION

2.1 Introduction

Segmentation of WBC has proven to be a complex task due to many reasons including presence of stains on the images acquired, cells overlapping, color similarities and non-uniformity of images.

Judging by previous studies, researchers had applied many algorithm to segment (WBC) from blood smear image as shown in table 2.1.

Table 2.1 Sample Segmentation of WBC from typical BC images

Typical BC image	Segmented WBC
	

Sabino and Costa [10] used the Green channel of the RGB model to segment WBC. On the other hand, Westpfalz applied HSI color model to separate WBC from background and de-cluster the clustered WBC [9]. Yang, Foran and Meer [12] improved the algorithm of IGDS to better segment WBC from other BCs presented in the smear image. They used LUV color model, color gradient and used “least square estimation algorithm” along with GVF snake algorithm. Sinha and Ramakrishnan [13] used color used HSI-equivalent of the WBC image, K-Means clustering followed by EM-algorithm to segment WBC along with the cytoplasm nucleus. Ongun et al. [14] used fuzzy patch labelling to segment WBC from other blood elements. Bikheth et al. [15] used Gray image of blood smears and hierarchical thresholdings improve further their ability to allocate and segment WBC.

2.2 Proposed Segmentation Methodology

To distinguish the different classes of WBC, the first step to be considered is to segment WBC and to separate them individually from the original blood smear image. Precise and powerful segmentation methods are mandatory to separate the WBC's. In this research RGB color model, Otsu's thresholding (Otsu's thresholding method is based on the thought of detecting a threshold value that minimizes the within class variance of resulting foreground and background classes) and Watershed Transform are used for segmentation [17, 18].

To ensure the effectiveness of each technique, pre-processing is performed on the captured images as presented in Fig.2.1.

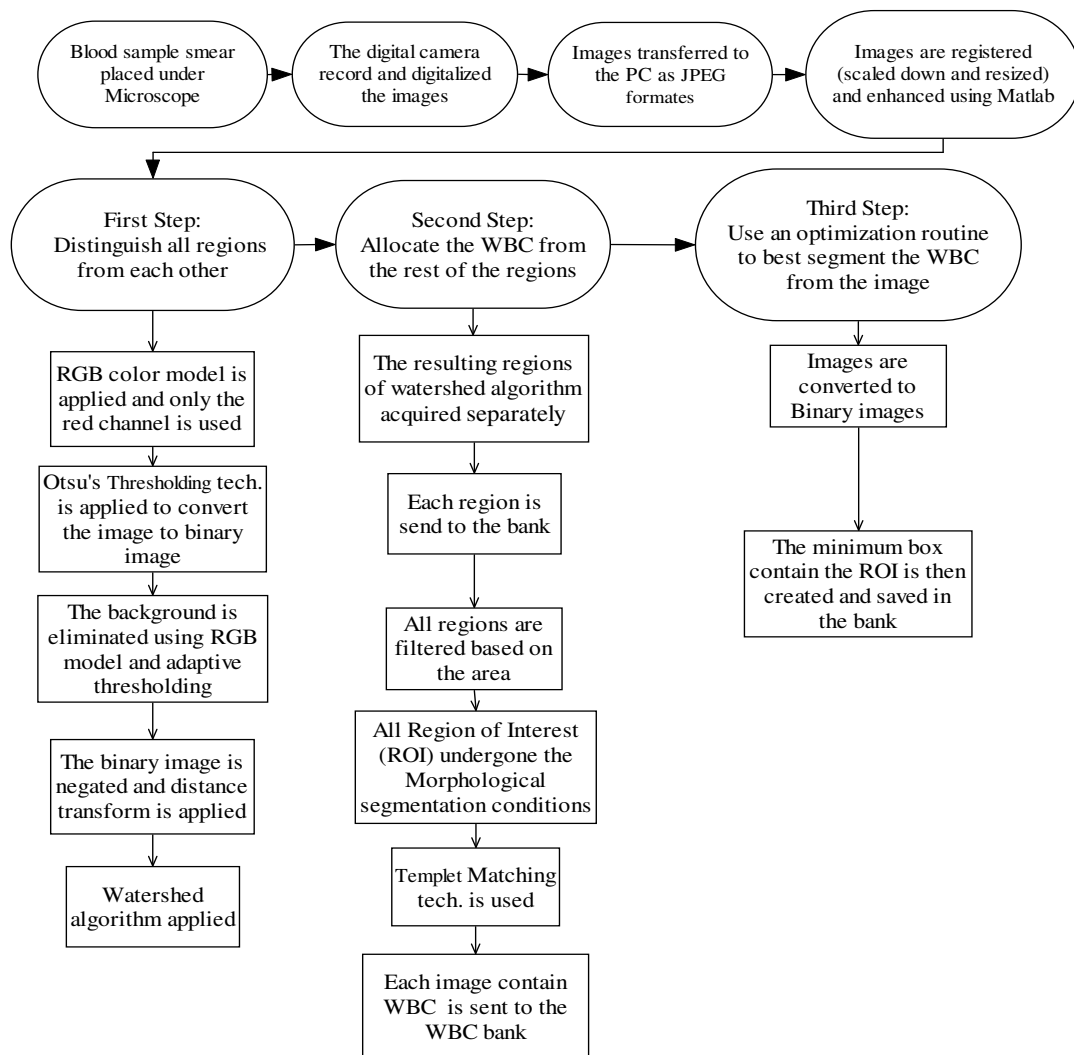


Fig. 2.1 Image acquiring, enhancement and segmentation flow chart (all concepts to be discussed further in the next sections)

Due to the fact that the elements of blood smears (WBC, RBC and Platelets) have lots of similar intensities, the problem of segmenting WBC from the digital image, realistically, is going to be a hard one. Also, each image has different segmentation's parameter values. In other words, the segmentation algorithm applied has to be retuned to each image in order to be able to segment WBC. Fig. 2.1 illustrates the proposed method adopted to reach the optimum segmentation, which will help automate WBC segmentation from blood smear sample image as follows:

- Distinguish all regions from each other
- Allocate the WBC from the rest of the regions
- Use an optimization routine to best segment the WBC from the image

Based on the above background, the processes followed to segment WBC are:

2.2.1 Image Gathering and Pre-Processing

Peripheral blood samples from 10 patients are collected and processed by Hematologist Department in Twam Hospital at Al-Ain in UAE. The hospital is mainly concerned with the diagnosis and treatment of cancer.

Images are captured from smear slides by an Olympus BX50 microscope, equipped with an Olympus color camera DP11. An 8-bit personal computer interface card is used to serially record data. For each image, the hematologist expert classifies WBC and these are recorded to build up the database (blood image and WBC presented type). Patients included are females and males with ages ranging from 24 to 55 years. The patients reported to the hospital are suffering from various degrees of illness (e.g. Leukemia, anemia...etc). The resolution of each image is 640 x 512 pixels and all images acquired are resized to (200 by 250) matrix to ensure standardization, save memory and process time. The registered images are sized down to reduce computational complexity and prevent region de-clustering especially when applying the watershed algorithm. For instance, for big objects the watershed transform segments the objects into many smaller regions. However, as the size of the objects is reduced, watershed transform algorithm will tend to skip smaller regions and make it more like one region.

During image acquisition, images are saved in JPEG format to use less computational requirements [19].

2.2.2 Pre-Segmentation and Thresholding

Fig. 2.2a shows a typical blood image. The image contrast is very low that the borders of the RBCs, WBC and platelets color close to background color. Red blood cells are clustered with white blood cells and the presence of noise, cell fragments and stains in the blood slides is significant. To overcome or reduce the effect of such factors, the images posteriori are standardized by means of increasing its contrast via applying histogram-stretching technique as the first pre-processing stage. Fig.2.2 shows the effect of applying contrast enhancement.

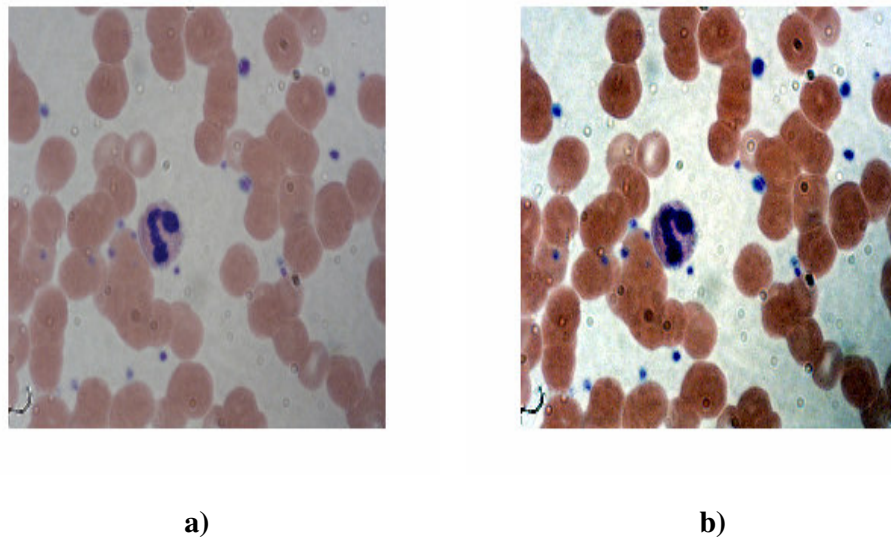


Fig. 2.2 Original images as captured from microscope b) Enhanced image color
In Fig.2.2, it is found that the applied “Intensity Adjustment”, which is a technique used for mapping image intensities values to a new range. Intensity adjustment algorithm is re-mapping the data values of a given image to fill the entire intensity range [0, 255]. The resulted image contrast then is increased (refer to Fig 2.2b). The ending result presents improvements in the boundaries of the objects; and made it more distinguishable (which is important when applying the segmentation technique).

The second pre-processing stage, involves minimizing the presence of other objects and grouping unwanted objects under different colors. Hence, various techniques are used to distinguish all regions from each other including image subtracting, Gray image, HSI color model and RGB color model.

Firstly, applying Image subtraction, the resulting image appears as shown in Fig.2.3.

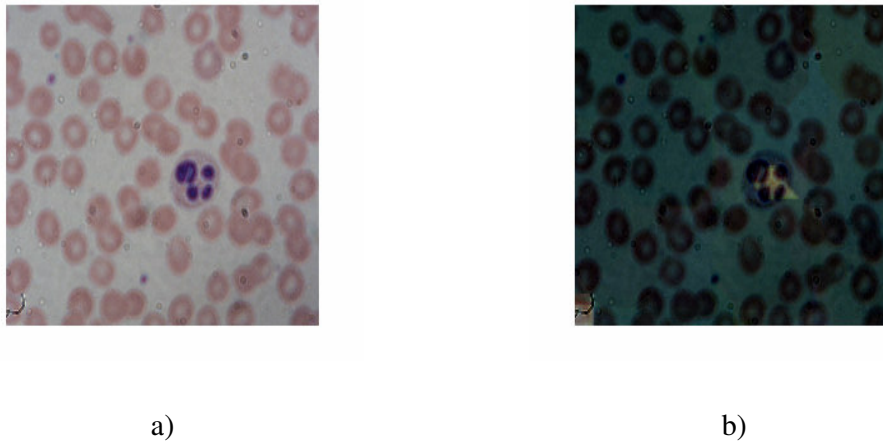


Fig. 2.3 a) Original image b) Image subtracted

Fig. 2.3 shows the image background subtracted from the original image. Although, it gives acceptable results in many applications [17, 18], in this application it is obsolete. The reason being that blood digital smear image objects, color contrast are very close to each other. Also, different objects share different ratios of red channel components.

Second, another approach that uses the Gray Image is adopted (This is the equivalent to a "Gray Scale Image"). It represents an image as a matrix in which every element has a value corresponding to brightness/darkness of each pixel). Fig.2.4b shows Gray image for WBC, where it is clearly shown that all RBC, WBC and platelets have almost the same color intensity.

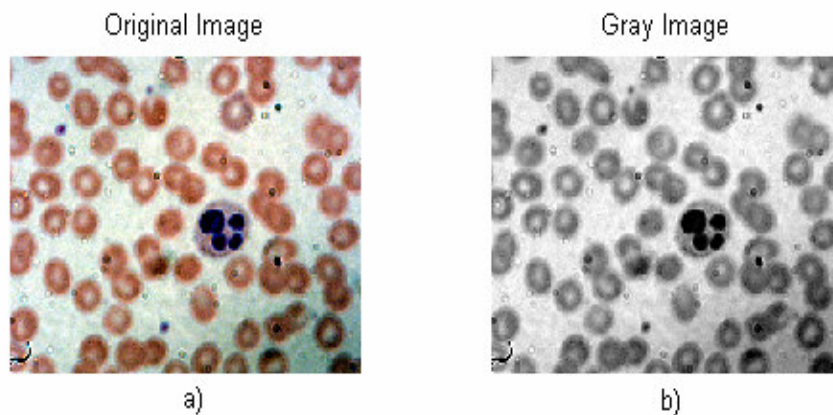


Fig. 2.4 a) Original image b) Gray image

Unfortunately, the Gray model does not present any variation between WBC and other blood components.

Third, HSI color model is used because it is found to be practical in some of the literature used. Fig.2.5 shows that the desired ROI WBC seems to be hard to be segmented from the rest of objects. However, the intensity channel is identical to the Gray Image shown in the previous image Fig2.4b.

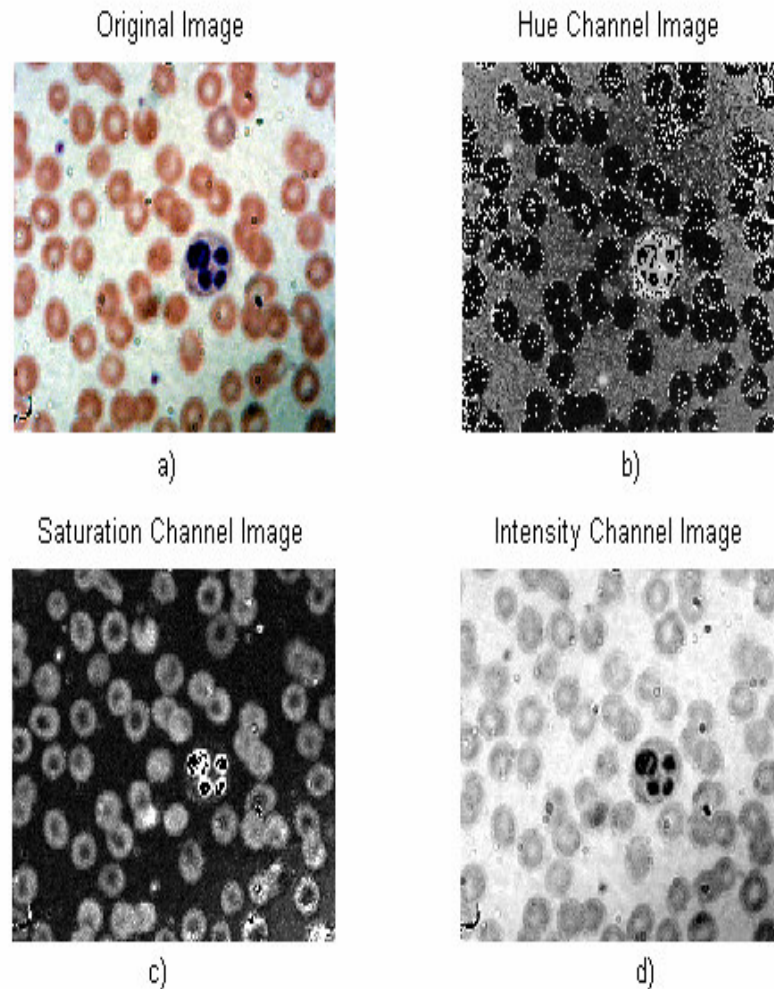


Fig. 2.5 a) Original image b) Hue image c) Saturation image d) Intensity image

Finally, RGB color model is used. Hence, it proves to be the best approach. The green and blue have not presented any tendencies to give the desired (ROI) WBC distinguish from the rest of the objects. In contrast, the red channel image seems to distinguish closely between (ROI) or the WBC and the rest of blood components.

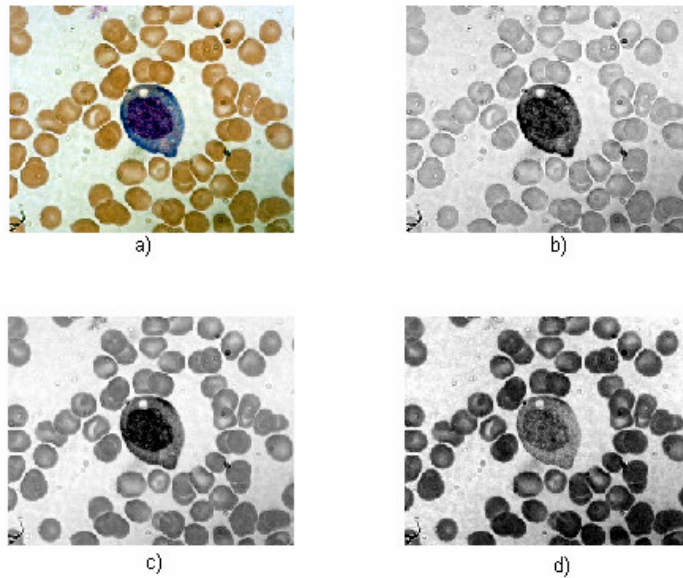


Fig. 2.6 a) Original image b) Red image c) Green image d) Blue image

To segment the desired WBC object from the background, it is found that the red component of the RGB input image gives the best contrast between the background and the blood cells components including WBC, RBC and platelets as shown in Fig. 2.6b. However, when the blue channel is used, WBC fades out as demonstrated in Fig. 2.6d. By applying the green channel the WBC cytoplasm color is close to the RBCs color as shown in Fig. 2.6c.

In the third pre-processing stage and in order to produce a representative binary image, Otsu's adaptive thresholding algorithm [20] is then applied on the red channel. Otsu's algorithm chooses the threshold to minimize the intraclass variance of the thresholded black and white pixels. The general mathematical model for the Otsu's threshold technique algorithm is:

$$\text{If } p(x, y) \geq T \rightarrow p(x, y) = 1 \text{ and this pixel belongs to objects} \quad (2.1)$$

$$\text{Else } p(x, y) < T \rightarrow p(x, y) = 0 \text{ and this pixel belongs to unwanted-objects} \quad (2.2)$$

Threshold technique is effective when the intensity levels of the objects fall squarely outside the range of levels in the background and the unwanted object levels, because spatial information is ignored, however, blurred region boundaries can create confusion. One of the main advantages of Otsu's method is that it is adaptive. That is for each

image, a different threshold is calculated to compute the ultimate global image threshold. Fig. 2.7c shows the output binary image produced corresponding to red channel image that was shown in Fig. 2.7b.

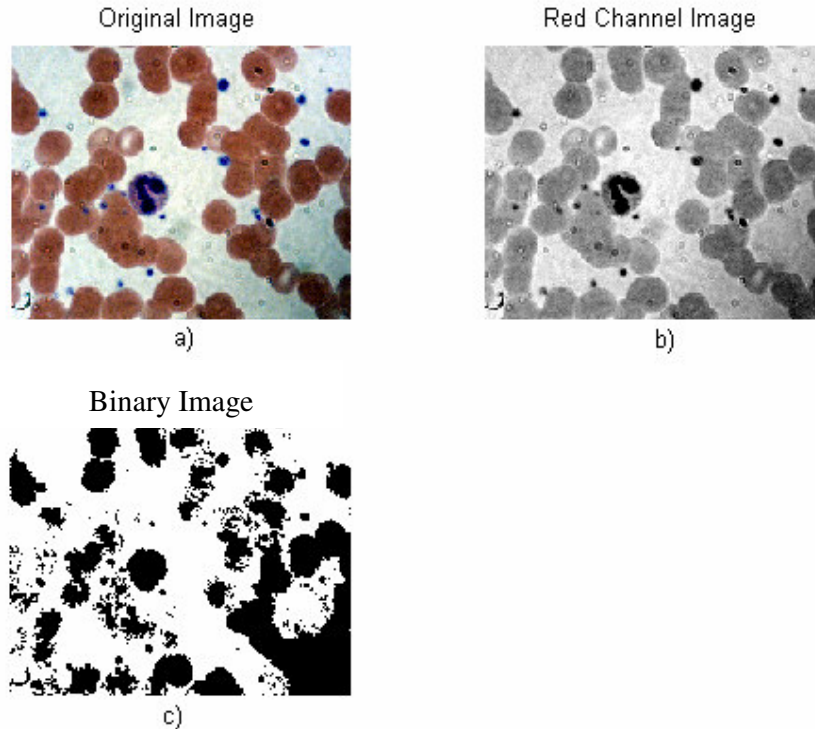


Fig. 2.7 Blood image after applying Otsu's adaptive

When Otsu's adaptive thresholding algorithm [20] has been applied on the red channel of the RGB image, the WBC is emphasized notably and the thresholding method is effective for all the images existing in the database.

2.2.3 Watershed Transformation and Region Properties

In the next stage of segmentation to distinguish WBC from the rest of the regions, watershed distance transform process is applied on the binary image obtained by Otsu's thresholding. The idea behind the watershed transform is to spot the local minimum which results after applying the inverse of distance transforms operation. Therefore, what is called a "Valley" is created and surrounded by the zeros (these are called "Watershed Pixels/Lines") [21]. These watershed pixels are the boundary of each object. Then, each region/valley is filled with a different color after being initiated by watershed algorithm from the center of the predefined valleys. As the regions grow, the nearby valley tends to

overlap. However, an elevated watershed lines is created to prevent overflow. This step ensures that each region is filled with different colors [22]. As a result, each group of nonzero values will be detected and will differentiate each region separately. At the center of the region it makes high pixel values and the pixel values converge to zero as the boundaries are approached. In other words as a pre-stage to apply the watershed algorithm distance transform, Otsu's output image is generated and processed by the watershed algorithm. Distance transform refers to computing the distance between each zero pixel and the nearest nonzero pixel in the binary image. This operation invokes the partitioning between the different regions by creating the valleys as stated before. It produces high pixel values at the centers of regions "center of valleys". Also, as the center of valleys approaches the boundaries, the values converge to zero.

Using watershed on blood slides, different objects (including WBC, RBC, platelets and stain), are extracted from the original image. Fig. 2.8 shows the results of the watershed algorithm when applied on the image shown in Fig. 2.7. As it can be seen, a considerably large number of segments is achieved while the image has only one WBC.

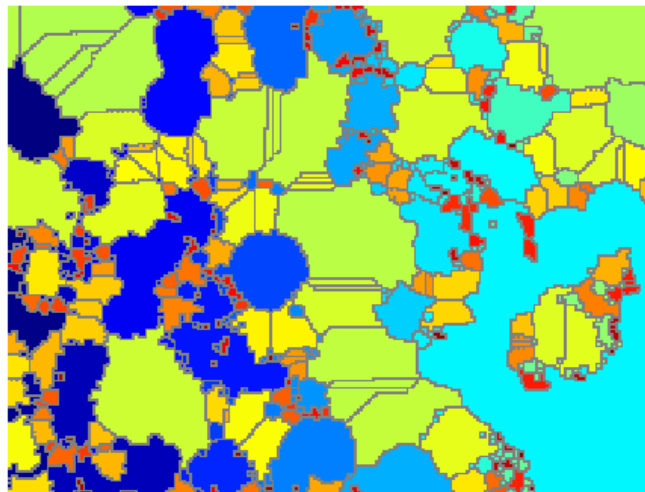


Fig. 2.8 Watershed output of the image shown in Fig.2.6b

2.2.4 WBC Detection and Post-Segmentation

At this stage a decision has to be made in order to figure out which masks, of the many obtained from watershed, represent WBC. Each area obtained with the watershed is singled out by masking it with the original image. Furthermore, a bounding box is created

to reduce the background part and better prepare the segment object for further processing. The main approach is based on mathematical computational segmentation. This means that the adapted algorithm should find parameters that differentiate the desired WBC from the blood image to be found. The first stage of WBC classification is based on the area of the bounding box representing each element obtained from watershed stage. Since WBC has distinctive area size when compared with other elements, a threshold value is obtained using trial and error approach.

The other two features that are used in the second stage to classify WBC from other objects where color averaging (A) and the aspects ratio (ASR) of the bounding box given as:

$$A = \frac{\sum_{x=0}^N \sum_{y=0}^M R(x,y) + \sum_{x=0}^N \sum_{y=0}^M G(x,y) + \sum_{x=0}^N \sum_{y=0}^M B(x,y)}{3} \quad (2.3)$$

$$ASR = \frac{N}{M} \quad (2.4)$$

Where N and M are the width and height of the bounding box in pixels of the region under consideration, R, G and B refer to RGB individual matrix values. Threshold values for the above two features are obtained for typical WBC and any bounding box that does not meet these thresholds conditions is then disregarded as being a WBC.

2.3 Results and Discussion

The initial database contains 120 Neutrophils, 96 Lymphocytes, 67 Eosinophils and 76 Monocytes WBC. Although other works in the area have incidentally found that the use of the intensity channel of HSI color model space gives adequate segmentation results [23], this work has shown that using the red component of the RGB model would give better uniformity for the background color as can be seen in Fig.2.9c. This would improve background eliminations using Otsu's adaptive thresholding algorithm.

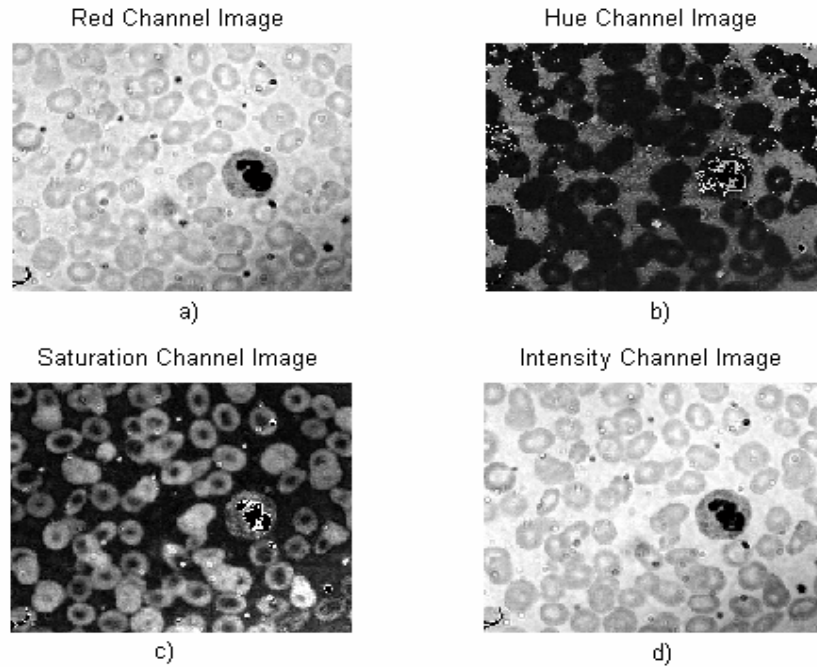


Fig. 2.9 RGB (Red Channel) and HSI model space channels comparison

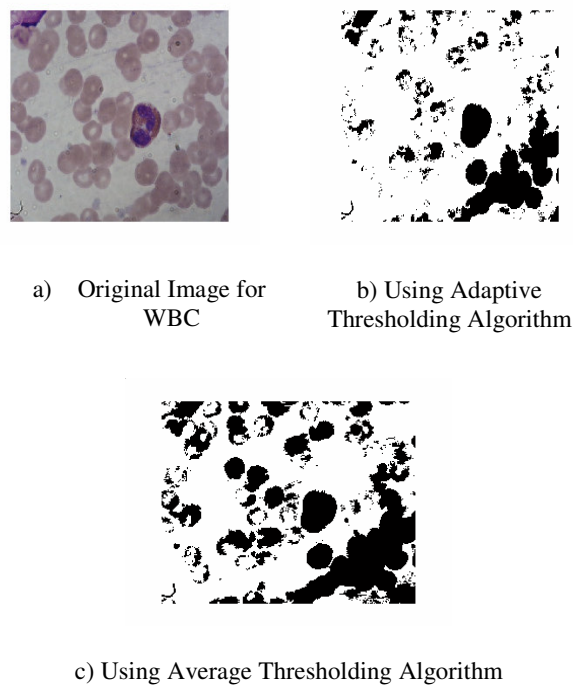


Fig. 2.10 Using the normal and the adaptive algorithm

Many threshold techniques are tested to convert the RGB image into a binary image. However, Otsu's method is found to give appropriate thresholding since each image had

different characteristics for many factors including storage time of slide, lighting level and stain degree. Fig. 2.10c shows the resulted images using average and Otsu's adaptive thresholding. As it can be seen adaptive thresholding is capable of eliminating (or reducing the size) of many other blood elements which are not WBC.

This work has shown that in some cases the watershed produced segments contained a WBC with a major portion of a neighboring RBC as shown in Fig. 2.11a. To eliminate this unwanted object, the S component of the YES model [24] is modified and used to enhance the contrast of the nucleus and cytoplasm of the WBC.

$$\begin{aligned}
 Y &= 0.253R + 0.684G + 0.063B \\
 E &= 0.5R - 0.5G \\
 S &= 0.25R + 0.25G - 0.5B
 \end{aligned}
 \tag{2.6}$$

Based on trial and error experimentally, it is found that the following improved S component gives adequate contrast (S component modified and renamed as F) by reducing the percentage of blue component:

$$F(x, y) = 0.25R(x, y) + 0.25G(x, y) - 0.45B(x, y)
 \tag{2.7}$$

For the image shown in Fig. 2.11a, applying equation 2.6 on each pixel of the image would produce the mask shown in Fig 2.11b. Multiplying the original image with its mask eliminates the neighboring, unwanted elements as shown in Fig.2.11c.

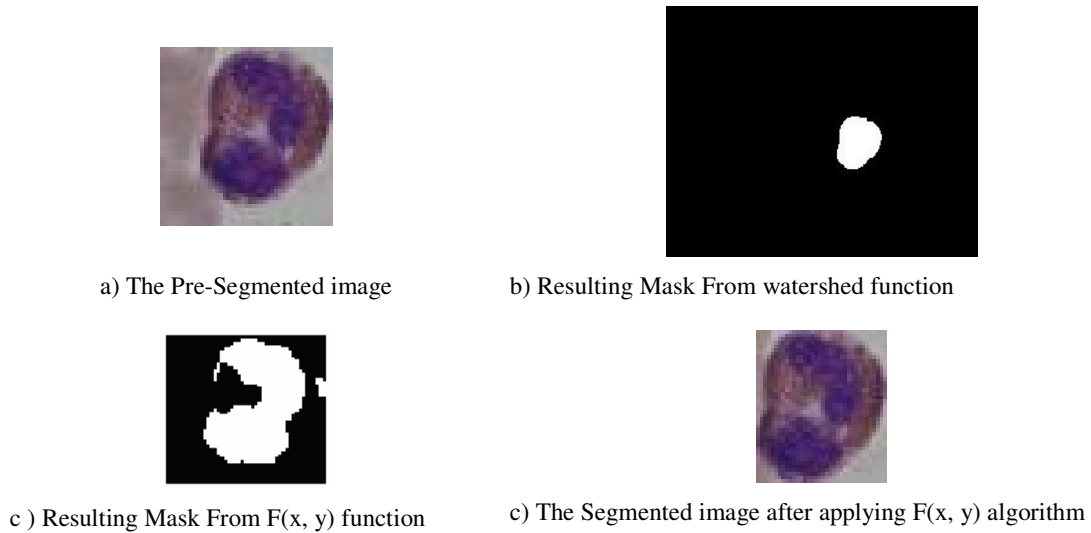


Fig. 2.11 Comparison between segmented images before and after applying equation 2.6

This concept is called “Template Matching Algorithm”. This can be interpreted as creating a mask for the wanted object and then place the mask on the blood image to mask out only the WBC cell presented in each smear image (by adding the masks of 2.11b and c, then multiplying the new mask with 2.11a to produce 2.11d). To have a measure of segmentation accuracy, a WBC is considered to be segmented accurately if the segment obtained by the proposed algorithm contains all the nucleus and cytoplasm and does not contain any full RBC or other objects. Table 2.1 shows the segmentation accuracy using the above discussed methodology (shown in Fig. 2.1).

Table 2.2 Segmentation accuracy for various types of WBC

WBC Type	Number of WBC	Number of WBC correctly segmented	Percent
Neutrophils	120	107	90%
Lymphocytes	96	96	100%
Eosinophils	67	30	45%
Monocytes	76	60	79%
Total	359	287	80%

Table 2.2 demonstrates the segmentation accuracy. Lymphocytes cells segmented properly and resulted in 100% performance. Neutrophils segmentation performance is reduced to 90% due to some cells’ borders are either clustered more with RBC or the borders are not well contrasted. With Monocytes, the algorithm achieved 79% because it faced the same problem as Neutrophil cell segmentation. Also, Monocytes cells cytoplasm is bright and this one of the limitation of the algorithm in terms of not being able to detect the bright boundaries. In case of Eosinophils, the segmentation algorithm achieved 45% due to Eosinophilis’s cytoplasm color which is similar to RBCs’ color.

As it can be seen from the above table, the Lymphocytes are better segmented due to the fact that cytoplasm and nucleus are clustered and cover all WBC making it easy for the watershed algorithm to contain it in one defined region. Fig. 2.12 shows correctly segmented Lymphocytes.

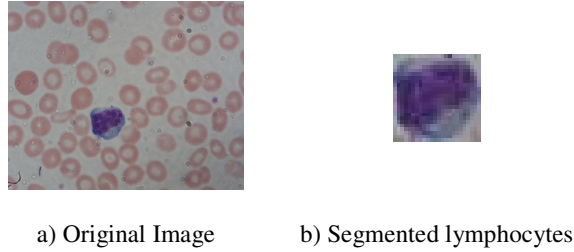


Fig. 2.12 Segmentation of Lymphocytes using the proposed method

However, inadequate performance is achieved for Eosinophils segmentation. As it can be seen in Fig. 2.12, adequate segmentation is achieved for some Eosinophils (Fig. 2.13a, b). However, in other cases a major portion of WBC is omitted (Fig. 2.13c, d). This could be due to the fact that, Eosinophils have red color WBC cytoplasm. Hence, when going through watershed WBC would be segmented to many regions. So, further work on this issue is needed.

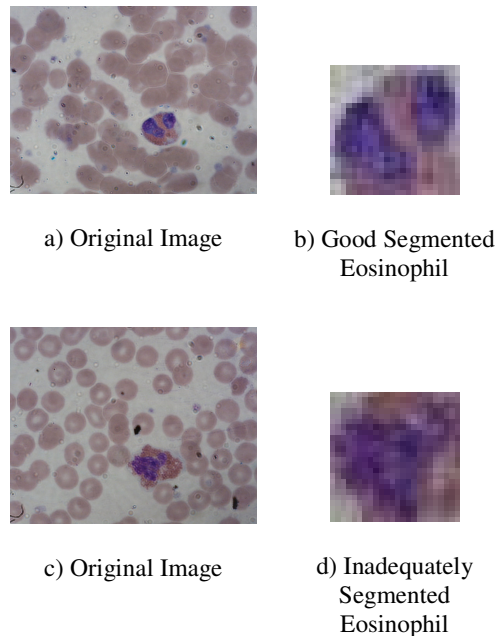


Fig. 2.13 Good and inadequate segmentation of Eosinophils WBC

In the segmentation part we can conclude the following:

- Direct segmentation technique is not useful when segmenting WBC.

- The proposed approach of segmenting WBC ensures only segmenting WBC rather than other objects such as clustered RBC, stains or cell fragments.
- The use of HSI color model, gray image and image subtraction have produce no adequate segmentation results in this study.
- As the size of the typical images of BC increases, over-segmentation will be presented if watershed algorithm is used.
- WBC allocation is very important in the segmentation of WBC due to the problem difficulty in terms of segmenting WBC.
- The segmentation part is free of parameter-tuning. Hence, the proposed methodology can deal with and segment all WBC images regardless of the time and microscope type used.
- Computational segmentation, region based and template matching are used for dynamic segmenting of all the WBC introduced in the blood slide smear image. This method helps tackle the problem of different color ratios between cells and image color intensity variation due to microscope or blood sample limitation.

The next step, WBC segmented images will be used to extract features that will help in classifying WBC classes.

CHAPTER 3

Feature Extraction

3.1 Introduction

To classify WBC, features that represent their images have to be obtained. Those features have to be capable of distinguishing between WBC classes (to be discussed further shortly); and it is desired to have as few features as possible. Although the classification accuracy is dependant on the classifier, the performance of the classifier is totally dependant on having adequate features.

Sabino and Costa [10] used features including: nucleus – cytoplasm ratio, perimeter, area of the nucleus and area of cytoplasm. Furthermore, they used GLCM as features which proven to be better in terms of supporting their classification arguments and got adequate results. Zheng et al [11] used images pixel intensity values as features and directly input them to NN to classify WBC images. Ongun et al. [14] extracted features from each (WBC) image such as morphological features (shape, color and texture features), shape features (areas of cell and nucleus cell perimeter, compactness...etc) and texture features (contrast, homogeneity...etc). Bikhel et al. [15] used the ratio of nucleus to cell area, circularity, measure average Gray level and area of nucleus and cytoplasm as features extracted from each (WBC) image. Park [16] feature vector consisted of shape, texture and statistical color features. Using these features, Park managed to get adequate classification accuracy of 70% using NN.


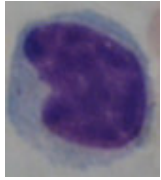

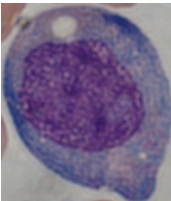
Feature extraction refers to finding common features in the Region of Interest (ROI) to classify it to classes. It is the objective of this work to find the minimum features required to classify four WBC classes shown in Table 3.1 as required by Twam Hospital's Hematologist Department. These classes are the main classes of WBC and they could change their formation based on their stage. The number of nucleus, color and WBC size play a major roles in determining the stage; and normality or abnormality of the WBC. In this work, the abnormal WBCs and Basophile WBCs are not considered because there is no enough image data available at Twam Hospital. A typical healthy blood sample will

have 7000-25000 of WBCs. However, in case of Leukemia for example, a blood sample drop could contain more than +50,000 of WBCs. A typical percentage for the distribution of the four types of WBC in a healthy person is as following:

<i>WBC Class</i>	Neutrophils	Lymphocytes	Eosinophils	Monocytes	Basophils
Population (%)	40 - 75 %	20 - 50 %	5 %	1 - 5 %	0.5 %

However, any major redistribution in the percentage could reflect a blood related medical problem. For example, if the percentages of Eosinophils exist in a blood sample is more than 5%, the person is suffering from some parasitic infection. Increase in presence of Neutrophil granulocytes may indicate bacterial infection. The higher presence of Lymphocytes indicates some viral infections such as glandular fever. Table 3.1 presents the importance of each class under study:

Table 3.1 WBC classes to be classified

Class Number	Class Name	Image related to each class	Description of Functions and importance to human body
Class 1	Neutrophils		<ul style="list-style-type: none"> • Produce enzymes which are a powerful anti-bacterial agent • Contain collagenase which help the cell move through connective tissue and lactoferrin (toxic to bacteria and fungi)
Class 2	Lymphocytes		<ul style="list-style-type: none"> • Generate specific immune response in the human body
Class 3	Eosinophils		<ul style="list-style-type: none"> • They increase greatly in many types of parasitic infection, allergic states, asthma and defence against the larvae of parasitic worms and unicellular organisms seems
Class 4	Monocytes		<ul style="list-style-type: none"> • Remove dead cell debris as well as attacking organisms such as Tubercule Bacilli (which causes TB) and some fungi

3.2 Types of Features

WBC features considered in this work can be classified into two types:

- **Morphological Features** including Geometric Features, Texture Features, Color Features and Shape based Features.
- **Spatial and Frequency Features** including Discrete Wavelets Transform and Discrete Cosine Transform.

Quantitative Analysis can be applied to get features that will help the intelligent software diagnose the class of the WBC sample Images. The following subsections include an illustration for the features, which are used to create Input-Feature-Vector (IFV) for the segmented WBC image.

3.2.1 Morphological Based Features

The morphological features considered in this work to classify WBC and their analysis are presented below:

Area (AR)

Area (AR) of the object is scalar and is calculated by counting the actual number of pixels in the region of interest.

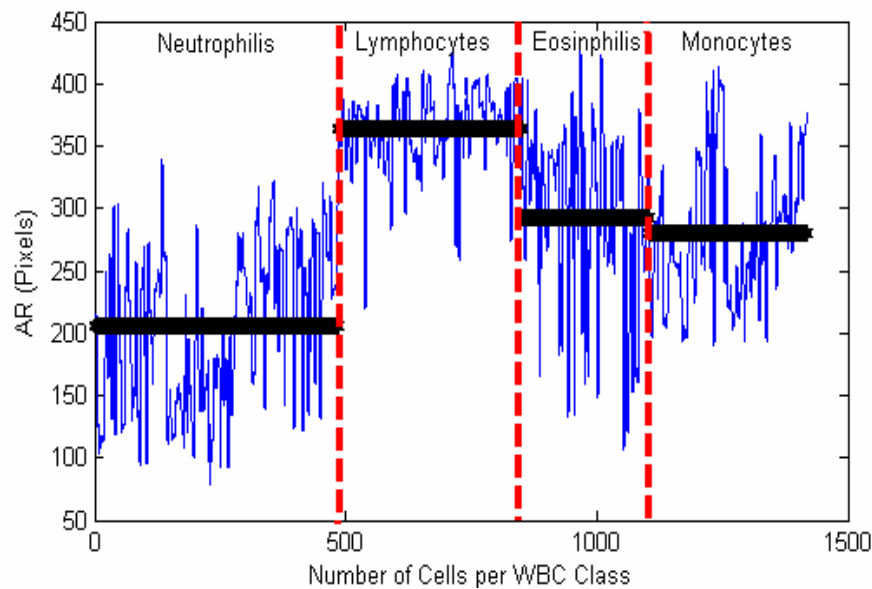


Fig. 3.1 Area of WBC

Fig. 3.1 shows the values of AR for all WBC in each class. The dotted lines represent class range separation. The thick lines represent the average of the values related to that class (to be called “average values”). The thin lines represent the real data calculated (to be called “feature values”). Although AR gives slight distinction between classes’ average values, class three and four are hard to differentiate. When looking at the WBC images, class four and class three of the acquired images tend to have same dimensions, whereas class one dimensions is different. The same conclusion could also be stated for class two.

Eccentricity (ECC)

Eccentricity (ECC) of the object is a scalar between (0 and 1), which describes the degree of similarity to a circle. If the object shape is very similar to a circle shape, then the object will have an eccentricity of 0. If the object shape is very similar to a line, it will have an eccentricity of 1.

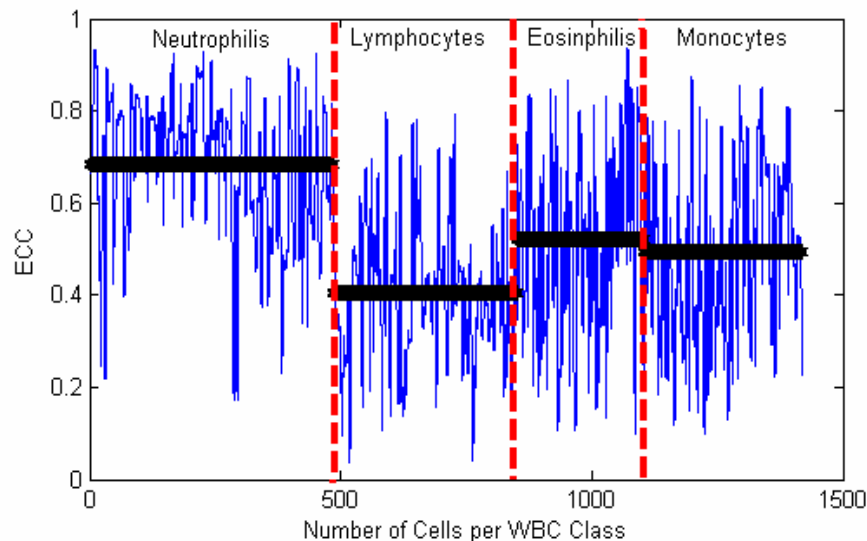


Fig. 3.2 Eccentricity (ECC)

Fig. 3.2 illustrates the ECC feature values and average features of each WBC group. The feature values and average value of class one is higher compared to other classes. However, the ECC for the other three classes are somewhat not that distinctive. When looking at the feature values, class one data had less overlaps with other class. Hence, ECC distinguished more class one.

Number of Objects (NOO)

Number of objects (NOO) is a scalar. NOO is the number of objects (Nucleus) produced in each WBC, which has to be fully separated.

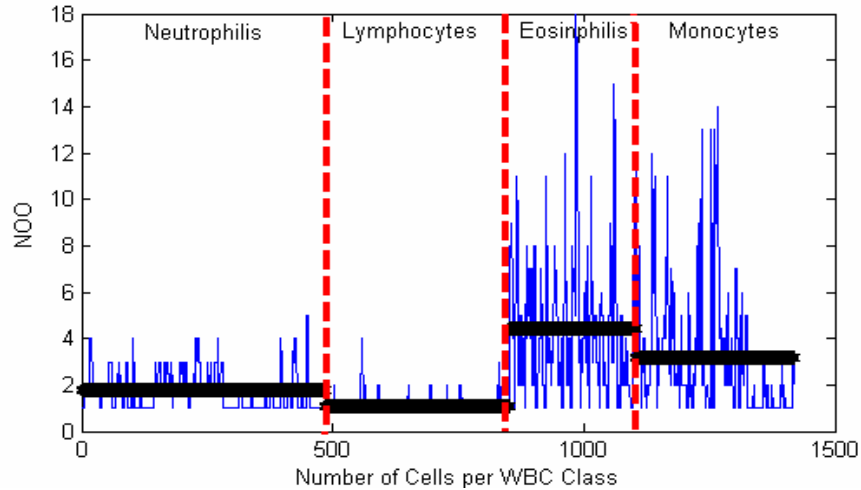


Fig. 3.3 Number of objects (NOO)

Fig. 3.3 shows the number of objects introduced in each WBC image per class. Class one and two had in average similar low number of objects. Similarly, class three and four have high and same number of objects. Therefore, NOO could differentiate class one and two from one side and class three and four on other side.

The Percentage of the Nucleus' Area to the Cell's Area of WBC (PNC)

The hematologist depends on PNC to determine the age and class of WBC. PNC is defined as following:

$$\text{Ratio of nucleus area to Cell area} = \frac{\text{Area of nucleus}}{\text{Total Area}} \times 100 \quad (3.1)$$

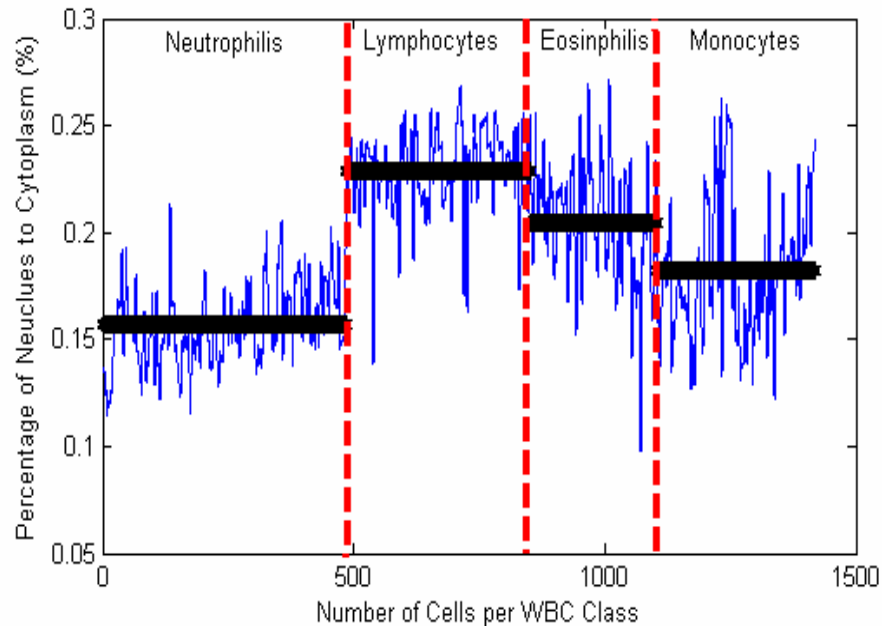


Fig. 3.4 Percentage of Nucleus to Cytoplasm (PNC)

Fig. 3.4 shows the PNC feature values and average values of each class. PNC average values give slight distinction between classes. By examining at class four, it is found that one group of monocytes has a similar feature of Lymphocytes and some Neutrophils. Considering the WBCs that of class 4 that had PNC feature values similar to class 2 as an example; and referring to Fig. 3.5, one can see the dimensions of both WBCs are the same. Hence, the stage in which these Monocytes at present made it, area-wise, similar to Lymphocytes cell, however, they are different in color only.

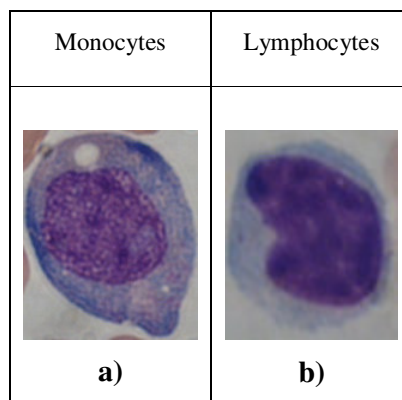


Fig. 3.5 a) Monocyte cell b) Lymphocyte cell

Although AR, ECC, NOO and PNC features could be used to distinguish between classes, outputs of the classifiers have shown inadequate classification accuracy could be

produced (30% - 63% classification accuracy). Also, it is found that when adding these features to other features (coming in the next sections) the classifiers (NN and PC) got confusing. The main reason for this low classification accuracy is that the above morphological features change as the WBC grow (as WBC grow in age, the morphology of the cell changes). For example, Monocytes in its early development stage are morphologically similar to Lymphocytes, but they have different colors. However, as the cell grows the morphological feature do change also. Hence, more WBC image data is needed to improve the classification accuracy of the geometrical based features.

Color Based Features

Color Features are proven to be one of the most promising features to segregate WBC classes in this research study; and the features used are as following:

First, Mean of color (x) intensity of the RGB model calculated as:

$$\text{Mean of (color x) channel} = \frac{\text{Sum of all (color x) Matrix Elements}}{1024} \quad (3.2)$$

Where x refers to RGB color channels (Red, Green and Blue) and the image matrix is sized as 32 x 32.

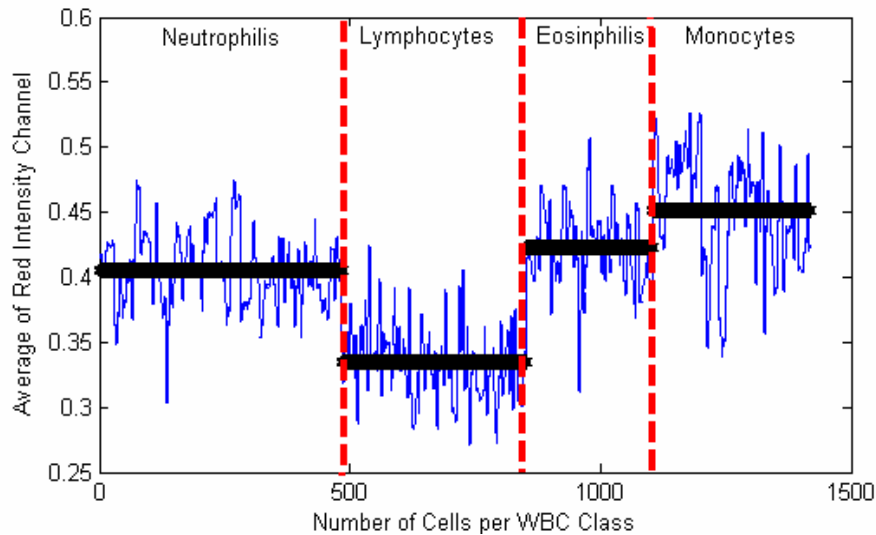


Fig. 3.6 Average Red intensity channel (Actual data and Average of the Actual data)

Fig. 3.6 shows the feature average and average values of the amount of red color in the four WBC classes. The figure, also, shows the average of Redness in each WBC group.

It can be seen that all classes have feature values that are considerably distinct between WBC classes. However, class one, two and three are overlapping.

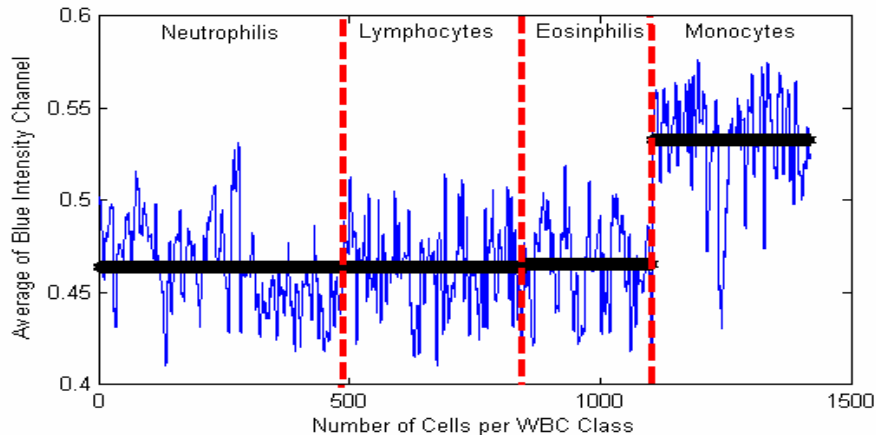


Fig. 3.7 Average Blue intensity channels (Actual data and Average of the Actual data)

Fig. 3.7 shows the feature average and average values of the amount of blue color in the WBC. The figure, also, shows the average of blue component in each WBC group. It could be seen that the blue intensity of class four is totally distinct from other classes.

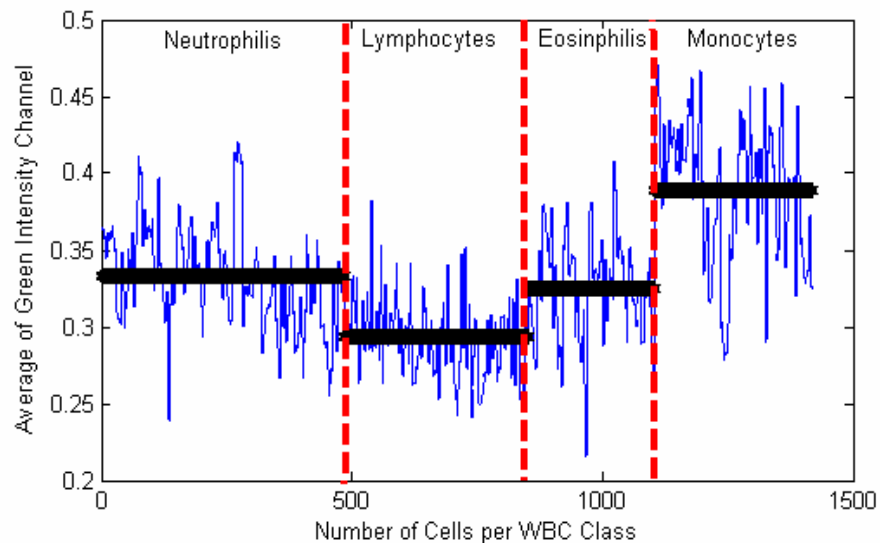
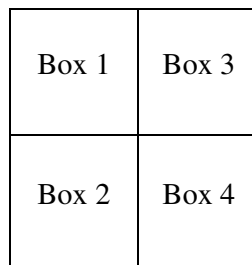


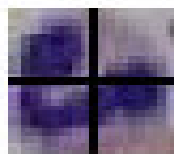
Fig. 3.8 Average Green intensity channel (Actual data and Average of the Actual data)

Fig. 3.8 shows the feature average and average values of the amount of green color in the WBC. The figure, also, shows the average of greenish in each WBC group. It could be seen that all classes had feature values were considerably distinct between WBC classes. But class one and four feature values share similarities in their values.

Another set of color features are obtained by dividing the image to four areas as shown in Fig. 3.9a and b. The average of each area is generated (each box pixels' average is calculated as shown in Fig3.9a). This feature vector is extracted from Red, Green and Blue color channels of each WBC image. The resulting feature vector contains twelve features.



a)



b)

Fig. 3.9 a) Image boxes b) Neutrophils image divided to four areas

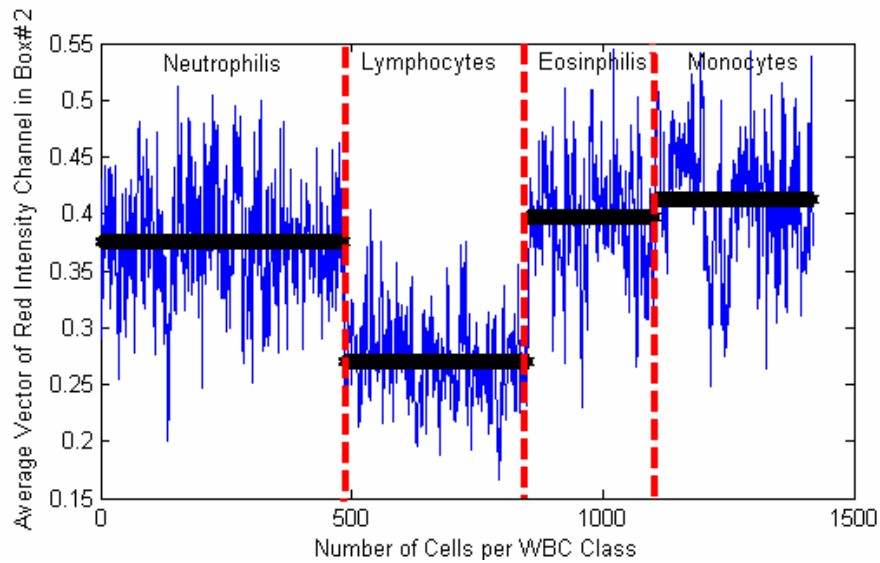


Fig. 3.10 Average of pixels' in box 2 per Red channel of the RGB color model

(Actual data and Average of the Actual data)

Fig. 3.10 shows sample feature values and average values per color channel for boxes 2 as an example. Slight class differentiation can be observed for all features values except for the feature values. The red component of box 2 distinct better class 2.

The color of nucleus is also considered. The WBC image is segmented to cytoplasm and nucleus. The average color of the nucleus only is considered. The following figure illustrates the outcomes.

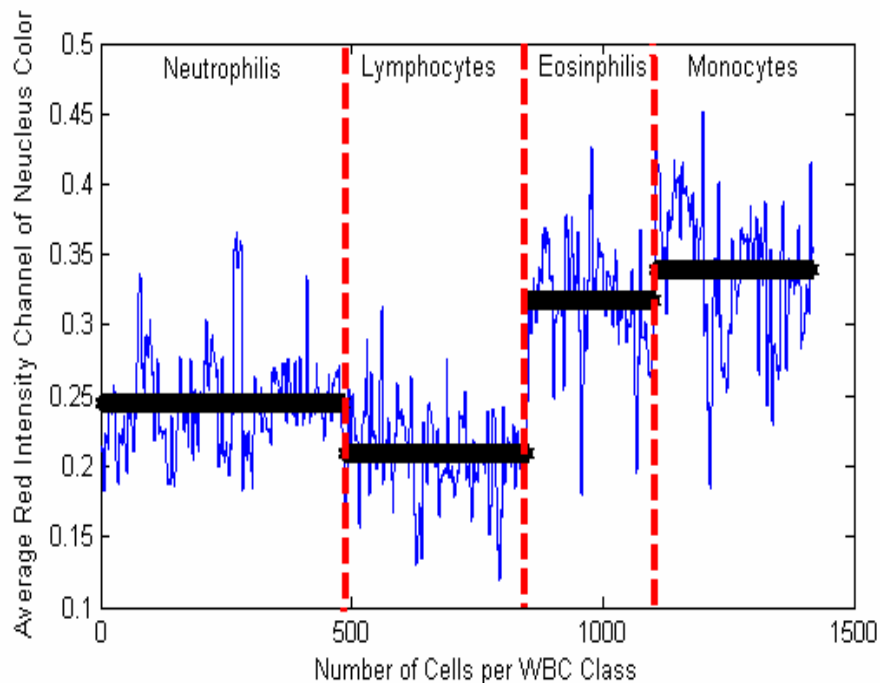


Fig. 3.11 Red Channel of Nucleus Color Average (Actual data and Average of the Actual data)

Fig.3.11 shows that sample of the red channel of RGB channel pixel average value. The feature values demonstrated slight distinct between WBC classes.

Morphologically speaking, some features are ignored since they add no extra value to the performance of the used classifier, give no adequate information, enlarge the size of feature input data and reduce the performance of the classifier. In the next chapter, all morphological features mentioned in this chapter will be examined to validate which feature to keep and which to eliminate.

3.2.2 Discrete Wavelet Transform Based Features

WT analysis uses basis function as Fourier Transform (FT) analysis and also based on decomposition of a signal using an orthogonal family of basis function. The most important advantage of WT compared to FT is that FT is practical in analyzing periodic and stationary signals. DWT is a transformation from spatial domain to frequency domain that can be used to analyze the temporal and spectral properties of non-stationary signals. WT is classified into Continuous Wavelet Transform (CWT) and Discrete Wavelet Transform (DWT) [25-28].

Multi-resolution theory is concerned with the representation and analysis of signals at more than one resolution. DWT offers better approximation at half the width and half as wide translation steps. The wavelet function Formula is:

$$W (j, k) = \sum_j \sum_k x(k).2^{-j/2} \psi (2^{-j} n - k) \tag{3.3}$$

Where $\psi (t)$ is time function with finite energy and fast decay called the mother wavelet.

DWT is seen as multi-resolution approximation expressions. Therefore, the signal analysis can be done at different frequency bands and different scales. Two channel banks low pass filter (G) and high pass filter (H) are needed to solve such multi-resolution analysis problem.

$$H[k] = \sum_n x[n]h[2k - n] \tag{3.4}$$

$$G[k] = \sum_n x[n]g[2k - n] \quad (3.5)$$

Consequently the resulting bank are down sampled by (1/2) of the previous frequency. This procedure is repeatable to obtain wavelets at any needed resolution level. In another words, DWT is developed to provide time-frequency information at various resolutions, which is a measure of the amount of detail information in the signal, levels of the image [28]. When DWT is applied to an image, the image will be divided into four sub images in which each image represents one resolution level. DWT is a discrete function, the “detail” and “approximation” coefficients from all resolutions are generated by convolving the image with Quadrate Mirror Filters (QMF) [4,13,20-22,26,28] see Fig. 3.12.

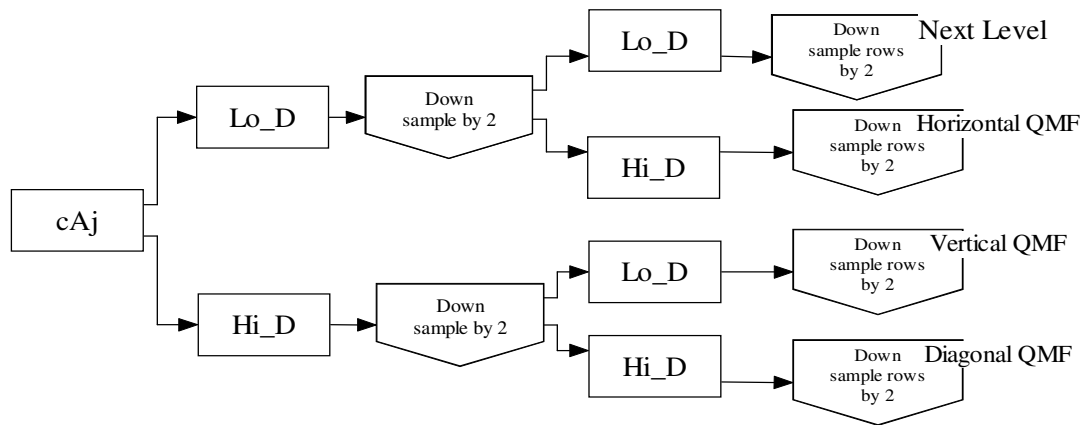
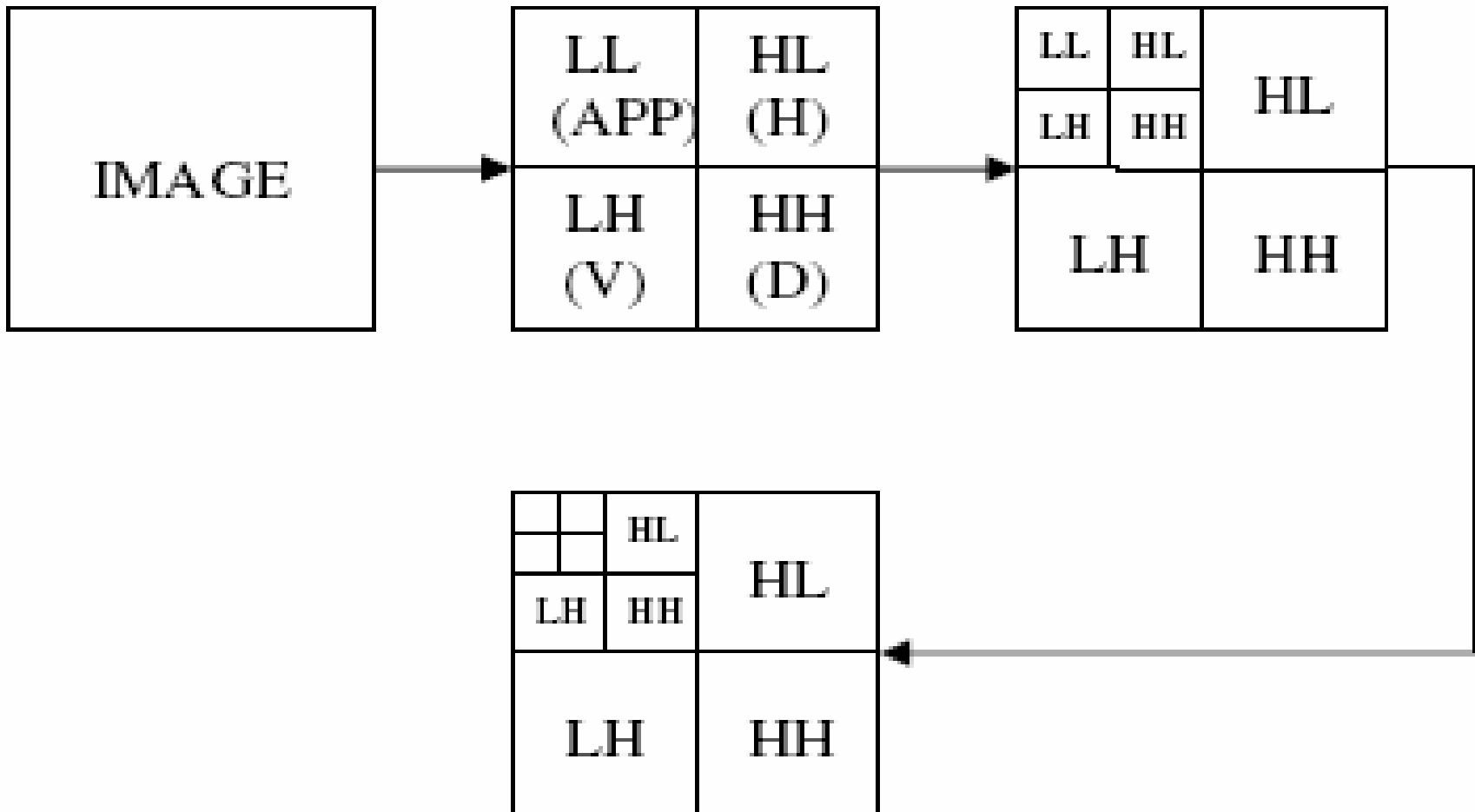
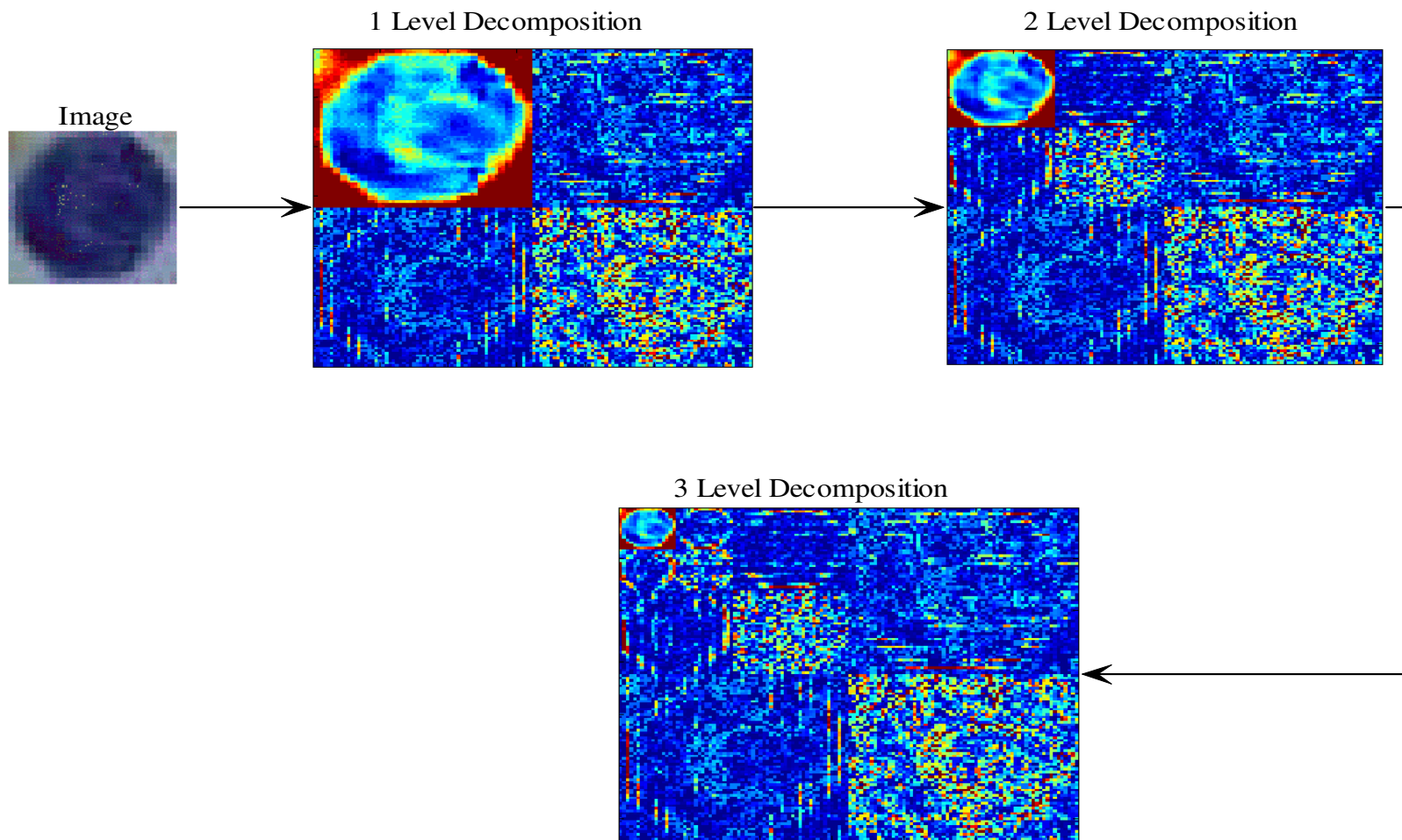


Fig. 3.12 Wavelets Coefficient [26, 28]

Those sub images correspond to low frequency variation (approximation coefficients) of the original image ($\mathbf{a(m,n)}$). The second, third and fourth resolutions level correspond to the high frequency (detailed coefficients) content on the vertical and horizontal and diagonal dimensions ($\mathbf{V(m,n)}$, $\mathbf{H(m,n)}$ and $\mathbf{D(m,n)}$) respectively, as depicted in Fig. 3.13.



a)



b)

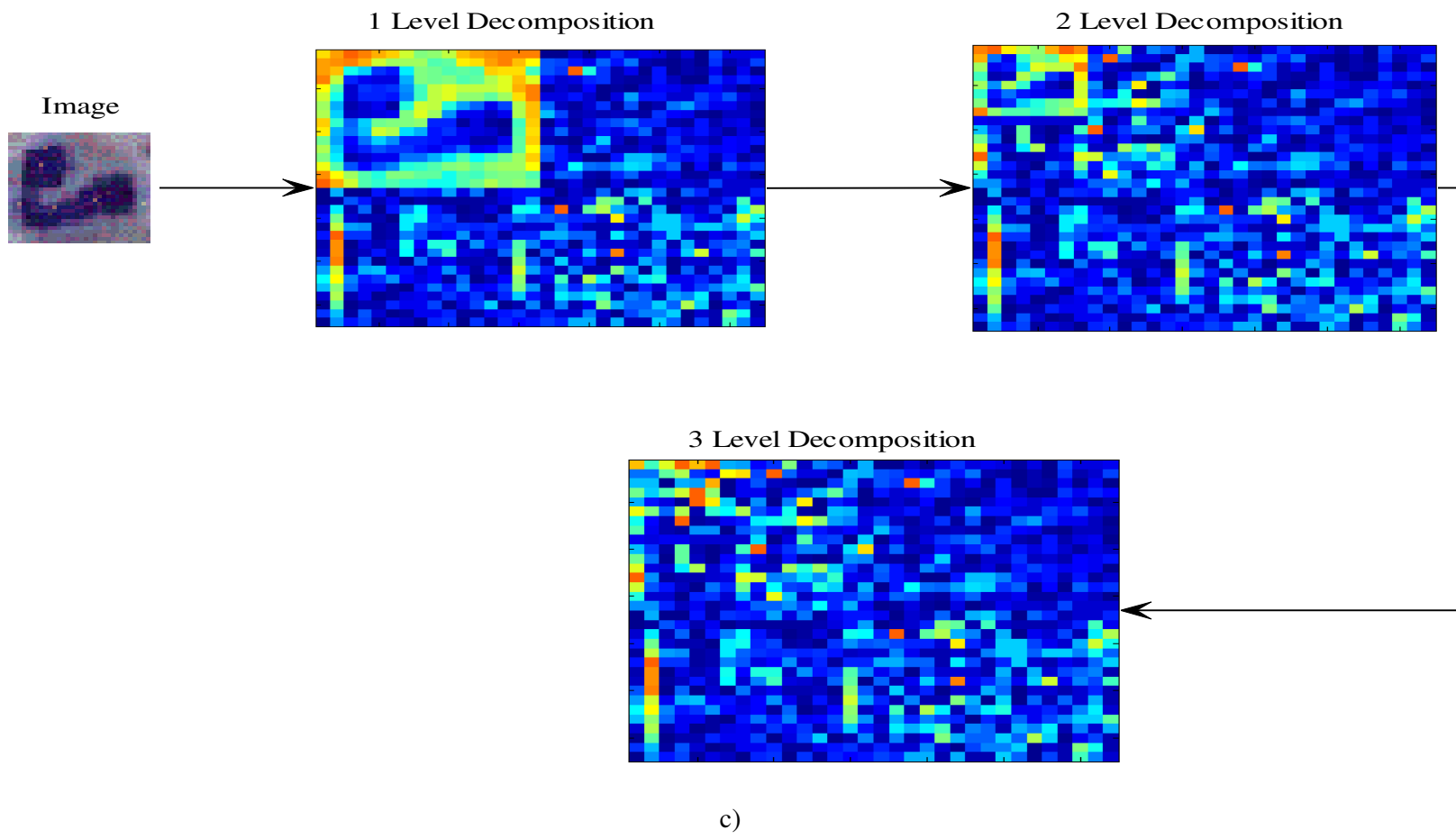


Fig. 3.13 a) Wavelets Decompositions up to 3 resolution levels b) Lymphocyte decomposition c) Neutrophil decomposition

As Fig. 3.13a illustrates, the following represents the name of the four sub images transformed from the original image [4, 28]:

- Sub-image “**LL**”: Both horizontal and vertical directions have low-frequencies.
- Sub-image “**HL**”: The horizontal direction has high-frequencies while the vertical has low-frequencies.
- Sub-image “**LH**”: The horizontal direction has low-frequencies while the vertical has high-frequencies.
- Sub-image “**HH**”: Both horizontal and vertical directions have high-frequencies.

Fig. 3.13 b and c show that most of the variation occurred in diagonal and approximation coefficients, whereas the horizontal and vertical coefficients do not give adequate variation. Hence, the average of the diagonal detailed coefficient at the various resolution levels is taken as features for classification as shown in Fig. 3.14.

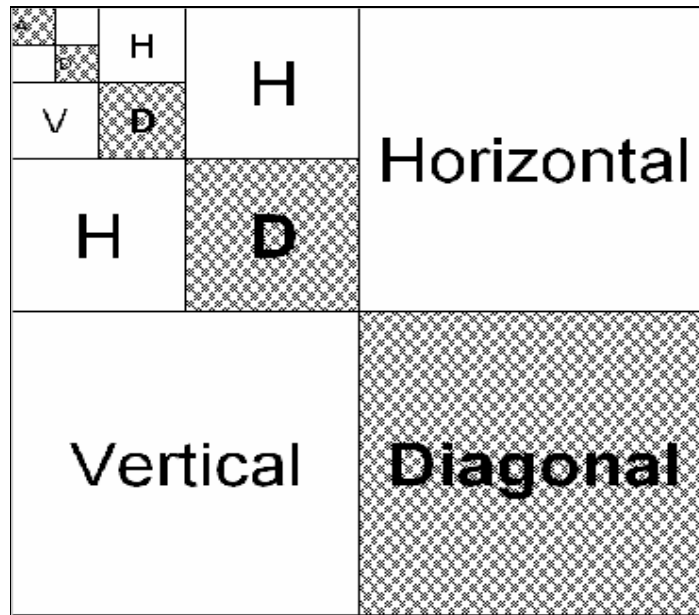


Fig. 3.14 DWT Image Structure Showing the Highlighting Diagonal and Energy coefficients

This feature is considered for red, green and blue color channels, but only the red channel has proven to give better results compared to other color channels.

Fig. 3.14 shows the WT coefficients considered of an image. The diagonal features are averaged per decomposition level (the highlighted boxes) and the same applied to the approximation coefficients. In Fig. 3.15 the average of diagonal coefficient is taken per level decomposition.

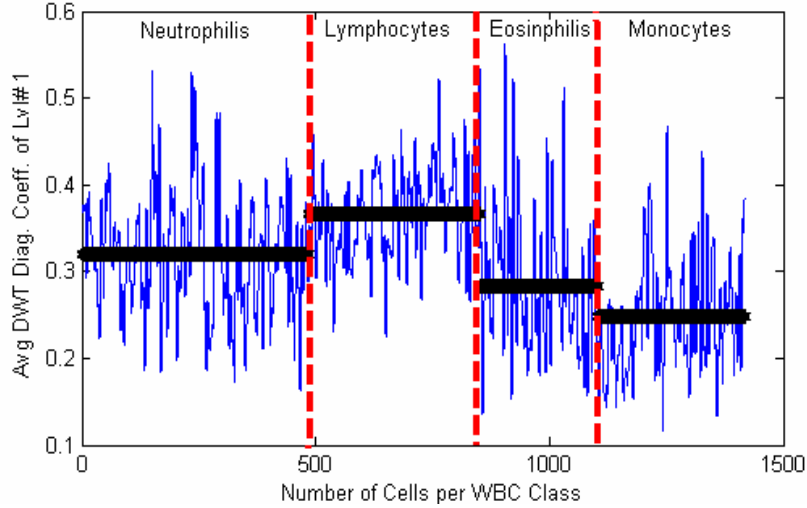


Fig. 3.15 Average of the diagonal coefficient using Haar Wavelets for the first resolution level (image is decomposed for 4 resolution levels) (Actual data and Average of the Actual data)

Fig. 3.15 shows sample diagonal detailed coefficients features for first resolution level data. The diagonal coefficients of level 1 have slight feature values distinction in all WBC classes.

3.2.3 Discrete Cosine Transform (DCT) Based Features

The DCT is a core technology used in image compression (e.g. JPEG) and video compression (e.g. MPEG). DCT is a Fourier-related transform and similar to the discrete Fourier transform (DFT), however, DCT uses real numbers only. In another terminology, DCT is a technique for converting a signal into basic frequency components. From the literature reviewed, DCT equation used for one Dimension is defined by the following mathematical equation: [28, 29]

$$y(k) = w(k) \sum_{n=1}^N x(n) \cos \frac{\pi(2n-1)(k-1)}{2N}, \quad k=1, \dots, N \quad (3.6)$$

Where

$$w(k) = \begin{cases} \frac{1}{\sqrt{N}}, & k = 1 \\ \sqrt{\frac{2}{N}}, & 2 \leq k \leq N \end{cases} \quad (3.7)$$

Where N is the length of x, and x and y are matrix of the same size.

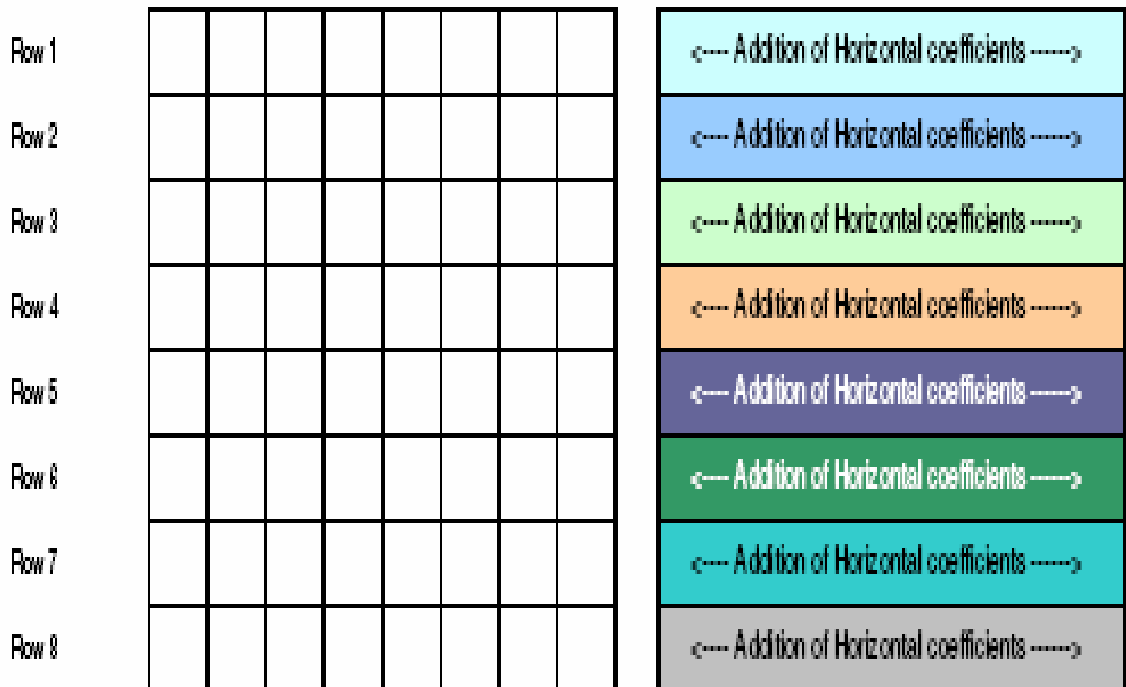
The mathematical equation used for images is shown [29]:

$$F(u, v) = \left(\frac{2}{N}\right)^{\frac{1}{2}} \left(\frac{2}{M}\right)^{\frac{1}{2}} \sum_{i=0}^{N-1} \sum_{j=0}^{M-1} \Lambda(i) \cdot \Lambda(j) \cdot \cos\left[\frac{\pi u}{2N}(2i+1)\right] \cos\left[\frac{\pi v}{2M}(2j+1)\right] \cdot f(i, j) \quad (3.8)$$

DCT is similar to the Fast Fourier Transform (FFT), but DCT can approximate lines well with fewer coefficients.

The two approaches used in this work to extract DCT features are as the following:

- **Averaging the horizontal information of the DCT coefficients.** Fig. 3.16 shows how the method is used.



a) WBC Image Matrix

b) DCT Coefficients Matrix

Fig. 3.16 Horizontal DCT Matrices of Coefficients

Thus, for (40x40) WBC image, a matrix vector of (1x40) is created by averaging each row separately. Then, each five rows are averaged again resulting in a matrix of (1x8) per color channel, RGB. Equation 3.9 demonstrates the mathematical formula used to generate row average:

$$f(m) = \frac{1}{40} \times \sum_{n=1}^{40} g(m,n) \quad (3.9)$$

Where m and n are the dimension of the matrix. f refer to the features retrieved per row. g refer to the matrix.

Fig. 3.17 describe the variation presented in the horizontal direction.

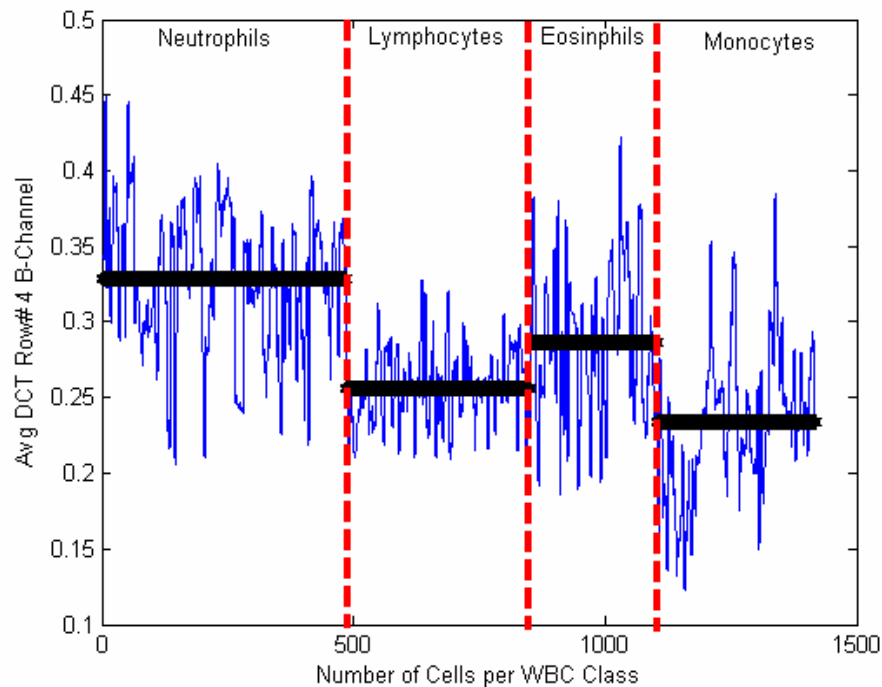


Fig. 3.17 Averaging the horizontal information of the DCT coefficients row # 4 (Actual data and Averages of the Actual data)

Fig. 3.17 demonstrates sample feature values and the average values of horizontal coefficients of DCT. The plot average value shows that there exists slight class differentiation between the different classes in DCT coefficients of “row# 4 blue channel” plot. However, the average values are showing slight distinction between the classes.

- **Blocks based on grouping features.** The information of the diagonal DCT coefficient is considered, Fig. 3.18 illustrates this grouping method for 8x8 image:

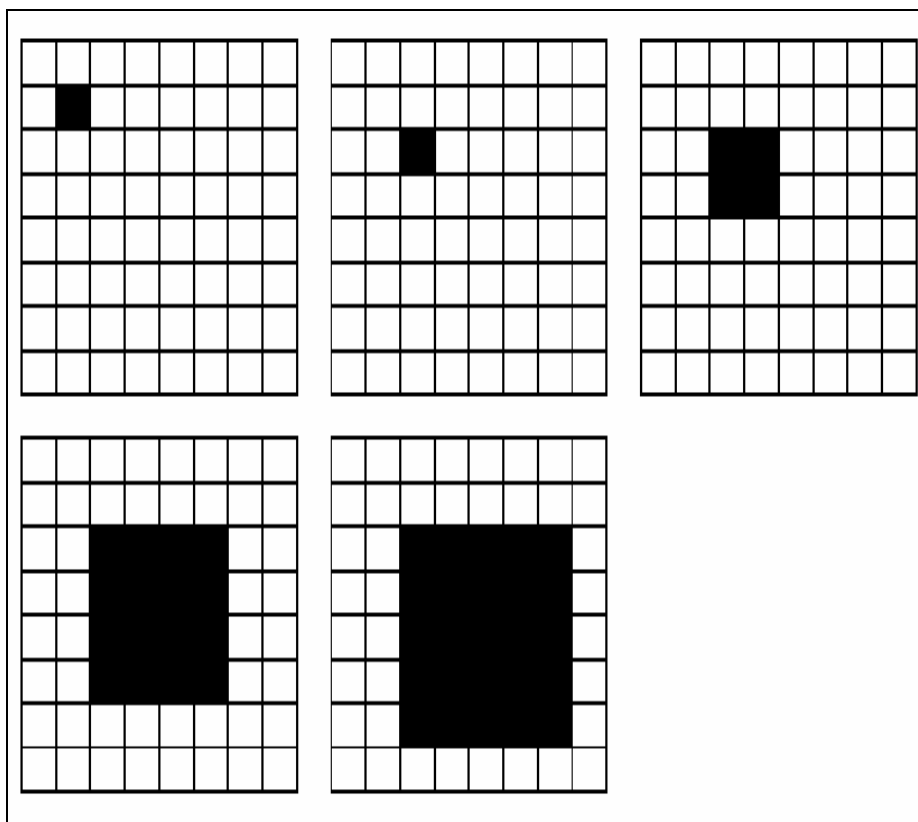


Fig. 3.18 Block based grouping of DCT diagonal coefficients

Fig.3.18 shows six matrices representing the image where the average of each DCT coefficient in each box gives a feature for classification. Applying this technique to WBC image resulted in a matrix consists of twelve features for Red, Green and Blue color channels (Four features per color channel). The reason for considering these area is because most of the information of WBC is concentrated in these area as highlighted in Fig. 3.18.

Typical values for the features obtained using this technique for boxes one and four (as an example) are shown in Fig. 3.19

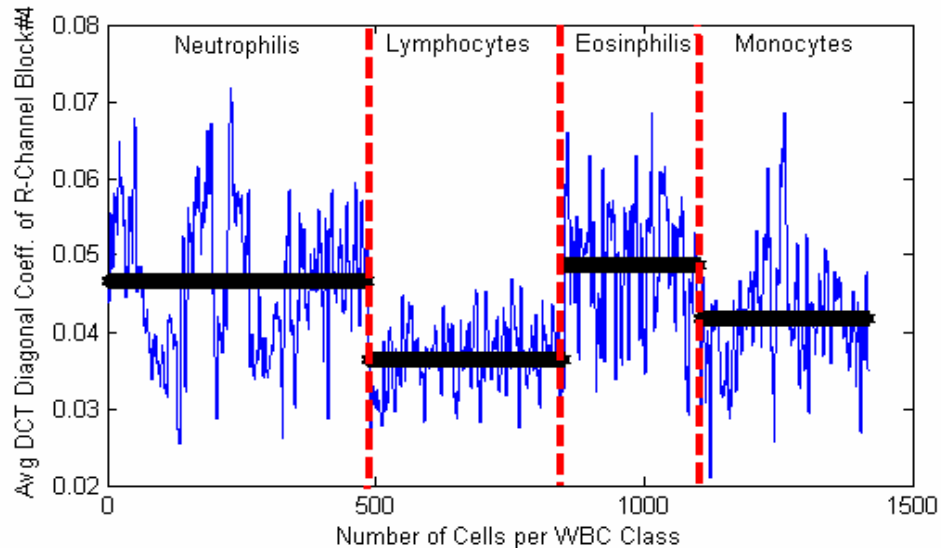


Fig. 3.19 Sample DCT average for the red component (Actual data and Average of the Actual data)

As can be seen from Fig 3.19, considerable distinction between WBC classes can be achieved using this feature.

Various modalities of morphological geometrical and shape features, color features, DWT features and DCT features would be used as an input feature vector to the classifiers in the next chapter.

CHAPTER 4

Classification

4.1 Introduction

Classification is a field that is concerned with grouping features into groups according to some classification values. There are many types of classifiers that can be used to differentiate objects such as finger prints, faces, white blood cells classes and more. When the class labels are known for a training set, the problem is considered as a supervised pattern recognition problem. Two classifiers are considered in this thesis. They are:

- Artificial Neural Network (ANN or NN)
- Polynomial Classifier (PC)

Classification based on Neural Network and Polynomial Classifiers represent the numerical approach to mimic human intelligent using a computer based machine. In Artificial Intelligence (AI) science, there exist different techniques for classification. NN is a technique that mimics the human natural brain's structure; recent studies are basing the classification upon statistical decision theory such as SVM or PC. Typical classifiers have either been based on either statistical methods or minimizing a mean-squared error criterion. All classifiers need training and testing phase which requires testing sets and training sets. During the training phase, the classifier is offered a set of feature vectors with known class label. During the testing phase, class label are determined for each presented feature vector.

The following two sections give brief background about both classifiers mathematical models. These two classifiers are then applied to the WBC type classification.

4.2 Classification Using Neural Network

Scientists have tried since the old days to discover how humans think. In the early 1940's scientists came up with the hypothesis that the brain consists of neurons which do the thinking operation. Based on that concept, they have developed and proposed a way to

mimic the human way of thinking using binary numbers which are the basis of Neural Network NN or Artificial Neural Network (ANN). A neural network [2] is a software (or hardware) replication of a biological brain. The principle behind neural network is to learn how to recognize patterns in a given set of data. Once the NN has been trained on samples of data, then NN will be able to make predictions by detecting alike patterns in upcoming data. The great advantage of NN is that it can detect similarities in inputs even if a particular input has never been seen previously. NN might detect important predictive patterns that are not previously apparent to a non-expert for the data stream under analysis. Therefore, NN can act and replace the field expert. As a result, NN is considered as a powerful tool for data mining applications.

Now, let us explore how NN works and to reveal the mathematics behind it [30,31]. Fig. 4.1 shows the structure of McCulloch-Pitts model. The Architecture of ANN consists of:

- Number of inputs and outputs of the network;
- Number of layers;
- How the layers are connected to each other;
- Transfer functions of each layer;
- Number of neurons in each layer;

Where (P) represents the inputs, (b) the bias, (f) the activation function, (W) represents the weight and (y) represents the (NN's) output.

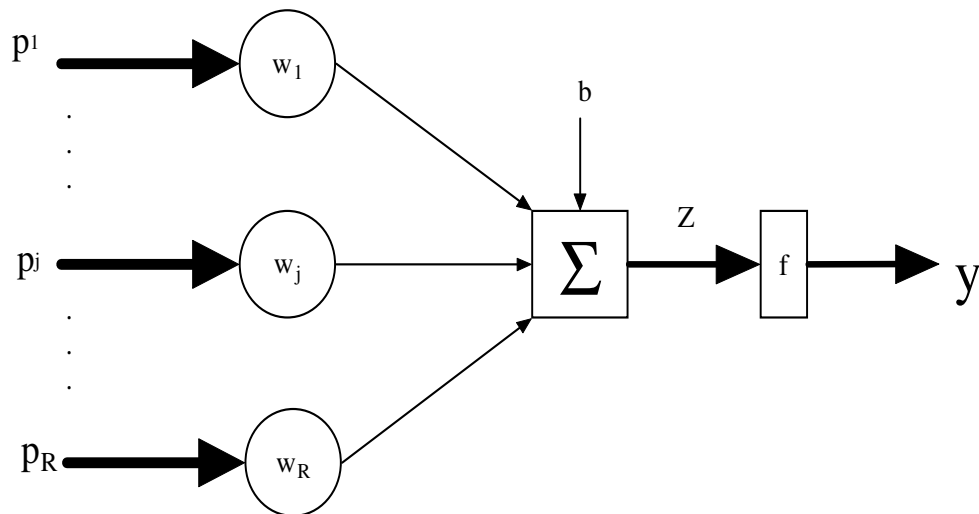


Fig. 4.1 McCulloch-Pitts model of an artificial neuron (Basic Model of Neuron) [30]

NN works in two directions (e.g. learning and testing). In case of learning or training, the network is fed with set of input examples and desired output. In the initial stage of running the NN, the output will be guessed for each given example. As stages reach stable levels after modifying the weights accordingly, NN will start to give satisfactory levels of output.

The output of NN can be calculated as follows [2,30,31]:

$$y = f(w_1.p_1 + \dots + w_j.p_j + \dots + w_R.p_R + b) \quad (4.1)$$

The general formula is

$$y = f(\mathbf{w} \cdot \mathbf{p} + b) \quad (4.2)$$

The Input Feature Vector (IFV) is used as an input to the system $\mathbf{p} = (p_1, p_2, \dots, p_R)$. Then, the desired output should be given. Each pair of neurons is associated with weight. Consequently, weights linked to the R th neuron can be represented as a weight vector of the form $\mathbf{W} = (w_1, \dots, w_j, \dots, w_R)$, where w_{iR} represents the weight associated with the connection between the processing element p_i , and the processing element p_R . When NN starts running, NN map input values to output/response values as a function of NN which is $y = f(\mathbf{p})$ (“ f ” is considered as the activation function).

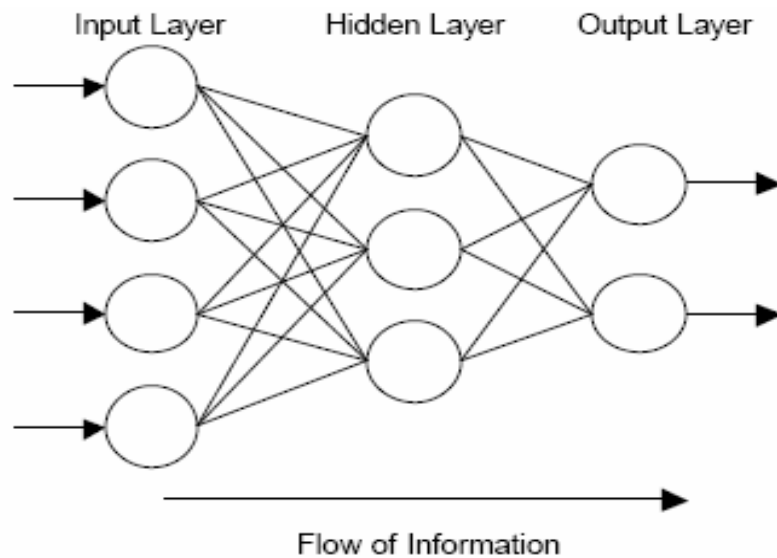


Fig. 4.2 General Structure for feed forward NN [2,30]

Fig. 4.2 shows the general structure for feed-forward NN network. The first layer is called “input layer”, the second is called “hidden layer” and the last layer is called “output layer”.

NN is (AI) software that is known for its ability to learn. For a given training set of input and output pairs where IFV represented by \mathbf{p} and the desired output, target value for y , represented by $\mathbf{t} = (t_1, t_2, \dots, t_R)$. Then, the learning rule calculates the updated value of the neuron weights and bias to minimize the gap between \mathbf{t} (the desired output) and y (the output of NN) as depicted in Fig. 4.3) [2,30,31].

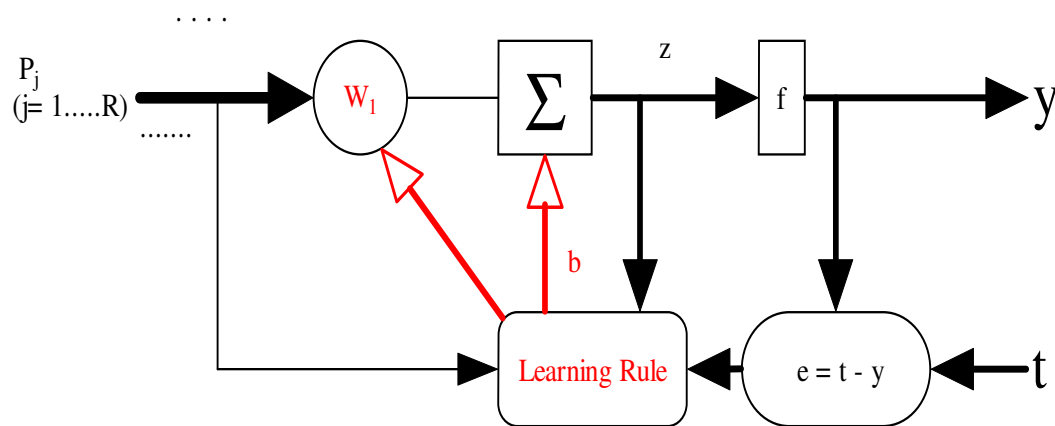


Fig. 4.3 Learning Rules (Training Algorithms) Diagram [30] (where z is the output of the sum of weights and bias)

4.3 Classification using Polynomial Classifier

PC is another type of (AI) that is used in pattern recognition problem [32, 33]. The polynomial classifier method operates in a similar way to the SVM with a polynomial kernel [32,33]. Polynomial Classifier can be viewed as input layer, the basis polynomial terms and the output layer. The indicated expression \mathbf{x} represents a feature vectors where $\mathbf{x} = (x_1, x_2, \dots, x_R)$ (x_1 represents the first feature in the feature vector and so forth). The vector $\mathbf{p}(\mathbf{x})$ consists of the polynomial expansion of \mathbf{x} , which represents the input vector introduced to PC. As a general rule, the polynomial basis terms are formed from the different set of products of the individual terms in the vector.

To train PC, the mean-square error criterion is used to produced the following

$$\mathbf{w} = \arg \min_{\mathbf{w}} E\{(\mathbf{w}'\mathbf{p}(\mathbf{x}) - y_c)^2\} \quad (4.3)$$

Where \mathbf{w} denotes to the optimum recognition model, y_c the ideal output (c the class label) and E refers to expectation over x and c .

Once the training feature vectors are expanded into their polynomial basis terms, the polynomial network is trained to approximate an ideal output using mean-squared error as the objective criterion

An output score is generated for each input vector, \mathbf{x}_i , by the inner product $\mathbf{w}'\mathbf{p}(\mathbf{x}_i)$. The total score as developed by Campbell and Assaleh [32-34]:

$$s = \mathbf{w}'\mathbf{p}(\mathbf{x}_i) \quad (4.4)$$

The IFV feature \mathbf{x} is rearranged in a matrix called \mathbf{A} . The matrix \mathbf{A} is of size $m \times n$ where m is the number of images and n is number of features \mathbf{x} . Each row in matrix \mathbf{A} represents the features extracted from each WBC image of a class C . The structure of matrix \mathbf{A}

$$\mathbf{A} = \begin{bmatrix} \mathbf{X}_1 \\ \mathbf{X}_2 \\ \mathbf{X}_3 \\ \mathbf{X}_4 \end{bmatrix} \quad (4.5)$$

Where \mathbf{X}_1 represents matrix of sets of features \mathbf{x} per WBC image of class $C=1$ and so forth.

From \mathbf{A} matrix, another matrix is extracted and called \mathbf{G} matrix. The generated \mathbf{G} matrix is of size $m \times n_{selected}$ where m is the number of images and $n_{selected}$ is the number of selected features \mathbf{x} . This matrix has same structure as \mathbf{A} except that the number of columns varies based on the number of selected features.

The target output $\mathbf{t} = (t_1, t_2, \dots, t_r)$ refers to the desired output of the polynomial classifier of size $i \times j$ where i is number of image and j is number of classes (the number

of classes is four classes). The elements of matrix \mathbf{t} are ranging from 0 to 1. The highest number in each row along with the location indicates the class number. For example $\mathbf{t} = [0.21 \ 0.14 \ 0.65 \ 0.8]$ the fourth column poses highest vales and this indicate that this is class four.

The polynomial expansion of that is derived from \mathbf{G} feature vectors is defined as

$$\mathbf{M}_i = [\mathbf{p}(x_{i,1}) \ \mathbf{p}(x_{i,2}) \ \cdots \ \mathbf{p}(x_{i,N_i})]^t \quad (4.6)$$

The global matrix for all C classes is obtained by concatenating all the individual \mathbf{M}_i matrices such as

$$\mathbf{M} = [\mathbf{M}_1 \ \mathbf{M}_2 \ \cdots \ \mathbf{M}_C]^t \quad (4.7)$$

Hence the output of the of the PC model is

$$\mathbf{O} = \mathbf{M} \cdot \mathbf{W} \quad (4.8)$$

Where \mathbf{W} is the PC weights and \mathbf{O} is the output matrix for all training inputs.

The solution of \mathbf{W} that minimizes the difference between $\mathbf{M} \cdot \mathbf{W}$ and \mathbf{O} is given by

$$\mathbf{W}_{opt} = \mathbf{M}^\dagger \cdot \mathbf{O} \quad (4.9)$$

The Moore-Penrose pseudo-inverse (symbolized by “ \dagger ”) of matrix \mathbf{M} is used to calculate the inverse of \mathbf{M} in equation 4.9 because \mathbf{M} is not square matrix.

CHAPTER 5

Results and Discussion of the Classification

5.1 Introduction

To classify WBC, Fig 5.1 illustrates the steps followed to develop a WBC differential system.

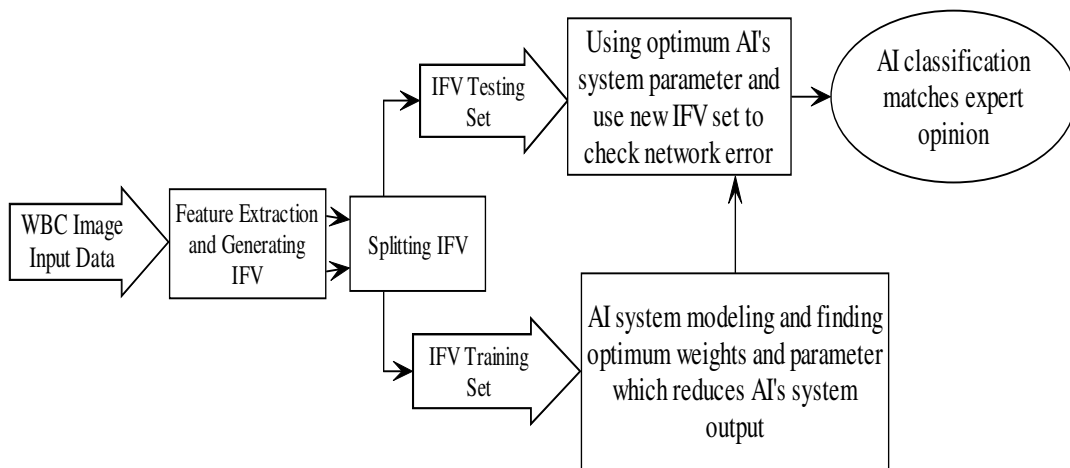

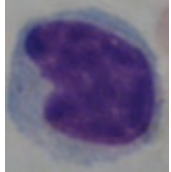

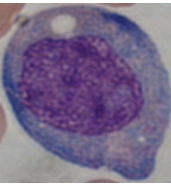


Fig. 5.1 AI System Basic

Based on Fig. 5.1, segmented WBC images are generated (chapter 2 covers capturing and segmenting of WBC from blood smear image). Then, IFV parameters are extracted from the WBCs segmented images (chapter 3 presents how features are extracted from the images). Subsequently, the resulting IFV of each group is divided to training and test patches. Next stage as Fig. 5.1 shows, the training patches are fed to the classifiers to train the classifiers and find a relation between the IFV and WBC class. Finally, classifiers will be fed with the testing patch to check if the classifiers can recognize the different various classes of WBC.

As a first step toward classifying WBC images, WBC classes are divided to four classes as stated previously. Table 5.1 shows the target value for the classifier output.

Table 5.1 Desired AIs classifier outputs for WBC classification

Output Classes		Image	Desired AI classifier outputs			
			O1	O2	O3	O4
WBC Classes	Neutrophils (class 1)		1	0	0	0
	Lymphocytes (class 2)		0	1	0	0
	Eosinophils (class 3)		0	0	1	0
	Monocytes (class 4)		0	0	0	1

After segmentation and feature extraction, the classifiers are fed with four sets of features as following:

- DWT
- DCT
- Morphological
- Combination of Morphological, DCT and DWT

The segmented images from chapter 2 (the adequate 80 % segmented images) is considered. Also, it is decided to manually crop the rest of the images to retain the database volume. The data is divided into two batches one for training the classifier while the other for testing them. The first batch consists of (708) segmented images of WBC and will be used for training the classifiers NN and PC. The second batch which consists of (716) segmented images will be used for testing the classifiers.

The following subsections summarize the outcomes of the conducted experiments using the above features.

5.1.1 DWT Based Classification

DWT is used to extracted features for each image (the first, second, third and fourth resolution level detail of the diagonal coefficients and approximation coefficients) as the Input Feature Vector (IFV).

Elements of IFV are Normalized based on two methods to minimize the feature data variation:

- Normalization by finding the maximum number per feature then dividing all raw by that maximum number. However, the classification result generated is poor compared to the second normalization method.
- Normalization using “**log**” function. In other words, the log of each feature is taken to form the feature vector. As a result, the final classification result has improved tremendously compared to the first method.

The Classification Accuracy (CA) for using NN with one hidden layer which consist of 40 neurons (using “logsig” activation function) and a second order PC is as shown in Table 5.2.

Table 5.2 Comparison between classifiers outcomes using DWT Features based on Haar with 4 resolution levels

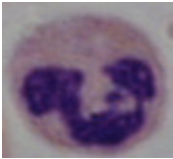
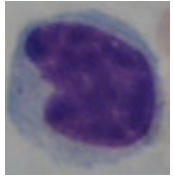

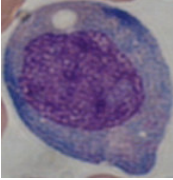
Class Number	Class Name	Image related to each class	Experiment 1 Classification Accuracy (%) (PC 2 nd order)	Experiment 2 Classification Accuracy (%) NN
Class 1	Neutrophils		65.16%	67.21%
Class 2	Lymphocytes		77.17%	71.20%
Class 3	Eosinophils		33.06%	40.32%
Class 4	Monocytes		46.95%	61.59%
Average			55.59%	60.08%

Table 5.2 shows the Classification Accuracy (CA) indicating the correctly classified WBC per class. The NN classifier gives around (60%) compared to PC which gives around (55%). These results are very poor. From the features data collected, the frequency changes in the diagonal coefficients are similar for most of the WBC images. This has resulted in confusing the classifier and led to poor recognition accuracy per class. Also, the number of levels is increased up to six levels, but the results did not improve because classes' misclassification increases due to more frequency overlaps.

It is found that not taking the approximation coefficients of the last resolution level resulted in low classification accuracy. This indicates that the low frequency information

is vital to give better classification. Although in average NN gives better class differentiation compared to PC, PC gives consistent and repeatable accuracy.

5.1.2 DCT Based Classification

Several approaches are used to extract features from WBC image after applying DCT algorithm. The two approaches to extract DCT features are as follows:

- **Averaging the horizontal information of the DCT matrix coefficients.**

Since the normalization of the log function gives better results in DWT, both methods are used to normalize IFV. However, log function demonstrates enhancement in the classification results.

Using these features as input for the NN and PC, Table 5.3 shows the outcomes of the resulting recognition accuracy (**in the following tables “√” indicates that the feature is selected, “X” indicates otherwise**). The choice of the feature is based on the result outcomes.

Table 5.3 DCT Data Sets of Horizontal Row Averaging

Experiment No. Input Feature Vector Components	Experiment 1	Experiment 2	Experiment 3	Experiment 4
DCT of Red channel (8 features)	√	√	√	√
DCT of Green channel (8 features)	X	√	X	√
DCT of Blue channel (8 features)	X	X	√	√

Table 5.3 shows the data sets combination used. Table 5.4 shows the resulting recognition outcomes for PC and NN.

Table 5.4 Comparison between Features outcomes via (PC and NN) classifier using DCT Horizontal Row Averaging


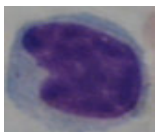
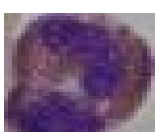
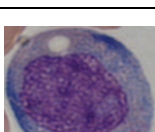
Class Name	Image related to each class	Classification Accuracy (%)							
		PC				NN			
		Exp 1	Exp. 2	Exp. 3	Exp. 4	Exp 1	Exp. 2	Exp. 3	Exp. 4
Neutrophils (Class 1)		77.9	74.6	78.69	95.9	70.4%	1.6%	67.6%	94.6%
Lymphocytes (Class 2)		90.8%	89.1%	87.0%	97.8%	58.6%	91.3%	58.1%	73.9%
Eosinophils (Class 3)		48.4%	54.8%	58.9%	75.8%	41.1%	41.1%	28.2%	87.9%
Monocytes (Class 4)		61.6%	64.0%	65.2%	87.2%	55.4%	3.6%	23.7%	90.2%
Average		69.7%	70.6%	72.4%	89.2%	56.4%	34.4%	44.4%	86.4%

Table 5.4 shows the CA of WBC class recognition. It can be seen that using the three colors DCT features give the highest CA percentage of 89.2% using PC. On the other hand, using NN produced a CA of 86.4%. The classification recognition for experiments 1-3 of each class is low especially for Eosinophils. One of the main reasons is that IFV parameter is not enough to recognize each class and it gets worse in case of Eosinophils. Also, DCT coefficient averages of each channel are overlapping. However, combining all the features allow the classifier to better recognize each class of WBC. In addition, the CA for Eosinophils has improved further due to the presence of more features which helps to better recognize this cell type. In other words, the increase in the number of features assist classifiers to figure out the patten related to each class. Also, the combination support classifiers to generate greater CA to that obtained by using DWTs' IFV.

- **Blocks based on grouping features.**

Block based on grouping features as mentioned in chapter 3, is another method of obtaining DCT diagonal block grouping features (see section 3.2.3 on page 42). This feature is calculated as shown in Fig. 3.18 in chapter 3 where the number of elements of in IFV is twelve.

The log function is applied to ensure the consistency of the features. These normalized features are fed to PC and NN, and the following feature combinations are arranged in table 5.5.

Table 5.5 DCT Data Sets of Block Grouping

Experiment No. Input Feature Vector Components	Experiment 1	Experiment 2	Experiment 3	Experiment 4
Block based grouping using DCT of Red Channel color (4 Features)	√	√	√	√
Block based grouping using DCT of Green Channel color (4 Features)	X	√	X	√
Block based grouping using DCT of Blue Channel color (4 Features)	X	X	√	√

Table 5.5 demonstrates the outcome of the classifiers used. The data is combined to cover all features possibilities and the outcomes are as the following

Table 5.6 Comparison between Block Features data sets as input to NN classifier


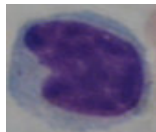
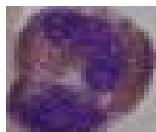
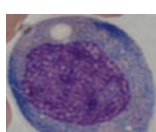
Class Name	Image related to each class	Classification Accuracy (%)							
		PC				NN			
		Exp. 1	Exp. 2	Exp. 3	Exp. 4	Exp. 1	Exp. 2	Exp. 3	Exp. 4
Neutrophils (Class 1)		84.8%	75.4%	66.4%	89.3%	74.5%	81.1%	84.4%	75.8%
Lymphocytes (Class 2)		87.5%	52.2%	47.8%	90.8%	84.6%	82.0%	78.2%	62.5%
Eosinophils (Class 3)		16.1%	21.8%	16.1%	77.4%	54.7%	61.2%	56.4%	40.3%
Monocytes (Class 4)		56.7%	31.7%	12.8%	71.3%	65.8%	68.2%	68.9%	34.1%
Average		61.3%	45.3%	35.8%	82.2%	70.2%	73.2%	72.0%	53.2%

Table 5.6 shows that an average accuracy of 70% can be achieved for one color or two color. Including a third color reduced the accuracy to 53%. However, including the data from three colors are necessary to achieve 82% accuracy with PC. Not doing that PC gives less accurate results CA result compared to NN. Since the classification accuracy of NN depends on various initial parameters such as network initial weights, which are chosen in random. The classification results are not repeatable. Hence, the average of many runs is to be taken to obtain a reliable performance measure.

The following summarize the above outcomes:

- The horizontal averaging of DCT coefficients provides better WBC classification when compared to block grouping.
- PC classification results are comparable with NN results. One of the reasons is that PC can tolerate the system non-linearity better than NN.

5.1.3 Morphological Based Classification

Morphological features are extracted from all WBC images as illustrated in Chapter 3. We extracted many features, but only color features proven to be best in assisting NN and PC classifiers to recognize each WBC class. When the geometrical features are fed to the NN, the classification accuracy is found to be 45%. But, when the same features fed to PC, the classification accuracy had improved and reached 58.32%, but these CA are poor and not considered further. The color based morphological features used for classification as shown in Table 5.7, which include total image average red, green and blue colors; average red, green and blue for the four dividers of the WBC image (see page 34); and the nucleus red, green and blue average colors. These features are normalized using the log function.

Table 5.7 Morphological Features modalities used per experiment

Experiment No. Input Feature Vector	Experiment 1	Experiment 2	Experiment 3	Experiment 4	Experiment 5	Experiment 6	Experiment 7	Experiment 8	Experiment 9	Experiment 10
Average Red Color (1 features)	√	√	√	√	√	√	√	√	√	√
Average Green Color (1 features)	X	√	√	√	√	√	√	√	√	√
Average Blue Color (1 features)	X	X	√	√	√	√	√	√	√	√
Average of Vector Red Channel (4 features)	X	X	X	√	√	√	√	√	√	√
Average of Vector Green Channel (4 features)	X	X	X	X	√	√	√	√	√	√
Average of Vector Blue Channel (4 features)	X	X	X	X	X	√	√	√	√	X
Average of Red Channel (Nucleus) (1 features)	X	X	X	X	X	X	√	√	√	√
Average of Green Channel (Nucleus) (1 features)	X	X	X	X	X	X	X	√	√	√
Average of Blue Channel (Nucleus) (1 features)	X	X	X	X	X	X	X	X	√	√

Table 5.7 shows IFV modalities used in each experiment. These modules are chosen on the basis of adding the feature which improves the classifier results. Also, individual features are tested but no promising results are generated. Using the IFV combination as illustrated in Table 5.7, the recognition results are shown in the following Table 5.8 and 5.9 for PC and NN respectively:

Table 5.8 Comparison between classifier and modalities features using PC based on morphological features

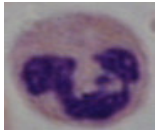
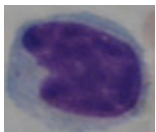
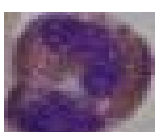
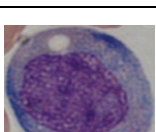

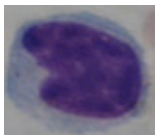
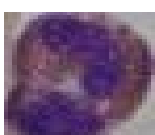
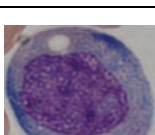
Class Name	Image related to each class	Classification Accuracy (%)									
		Exp. 1	Exp. 2	Exp. 3	Exp. 4	Exp. 5	Exp. 6	Exp. 7	Exp. 8	Exp. 9	Exp. 10
Neutrophils (Class 1)		83.2%	84.0%	85.7%	87.3%	94.3%	99.2%	99.6%	100%	100%	100%
Lymphocytes (Class 2)		82.6%	84.2%	95.7%	97.3%	99.5%	98.9%	100%	99.5%	98.9%	99.5%
Eosinophils (Class 3)		13.0%	52.4%	59.7%	65.3%	68.5%	80.6%	89.5%	91.1%	92.7%	91.9%
Monocytes (Class 4)		53.7%	63.4%	89.0%	90.2%	94.5%	94.5%	98.2%	99.4%	99.4%	100%
Average		58.1%	71.0%	82.5%	85.0%	89.2%	93.3%	96.8%	97.5%	97.8%	97.9%

Table 5.9 Comparison between classifier and modalities features using NN based on morphological features

Class Name	Image related to each class	Classification Accuracy (%)									
		Exp. 1	Exp. 2	Exp. 3	Exp. 4	Exp. 5	Exp. 6	Exp. 7	Exp. 8	Exp. 9	Exp. 10
Neutrophils (Class 1)		84.84	78.28	71.31	52.87	92.13	72.05	78.85	37.05	77.54	83.99
Lymphocytes (Class 2)		74.2	92.07	76.52	77.93	76.63	77.93	80.65	96.96	97.28	85.14
Eosinophils (Class 3)		12.74	65.00	61.45	80.00	57.42	75.00	55.32	85.97	89.68	78.17
Monocytes (Class 4)		55.00	64.88	95.00	94.88	92.20	92.07	98.17	75.61	96.71	75.45
Average		56.70	75.06	76.07	76.42	79.59	79.26	78.25	73.90	90.30	80.69

By comparing the results of Tables 5.8 and 5.9, one can see that the performance of PC increased as the number of features increased. PC gives recognition accuracy of (97.9%) by using all features except “Average of Vector Blue Channel”. Meanwhile, NN performance is less than that of PC where the best results are obtained and achieved CA of 90.3% using all features. When classifiers recognize Eosinophil, they produce low CA percentage especially at experiment one. As the number of features increases, classifier ability to recognize Eosinophil increases. The reason for this is that many Eosinophil images’ IFV parameter is overlapping with feature parameter of other classes. Enlarging the IFV allow more ability to recognize Eosinophil.

5.1.4 Combination of Morphological, DWT and DCT Features for Classification

This step is essential because each of the classifiers outcomes, presented in previous subsections, managed to reach acceptable classification results. In order to enhance the recognition accuracy one step further, morphological, DWT and DCT features are combined as the Table 5.10 shows.

Table 5.10 Data Sets used for the combination of features

Experiment No. Input Feature Vector Components	Experiment 1	Experiment 2	Experiment 3	Experiment 4	Experiment 5	Experiment 6	Experiment 7	Experiment 8	Experiment 9	Experiment 10	Experiment 11	Experiment 12	Experiment 13	Experiment 14	Experiment 15
Average Red Color (1 features)	√	√	√	√	√	√	√	√	√	√	√	√	√	√	√
Average Green Color (1 features)	√	√	√	√	√	√	√	√	√	√	√	√	√	√	√
Average Blue Color (1 features)	√	√	√	√	√	√	√	√	√	√	√	√	√	√	√
Vector of Average Red Channel (4 features)	√	√	√	√	√	√	√	√	√	√	√	√	√	√	√
Vector of Average Green Channel (4 features)	√	√	√	√	√	√	√	√	√	√	√	√	√	√	√
Vector of Average Blue Channel (4 features)	X	√	√	√	√	√	√	√	√	√	√	X	X	X	√
Average of Red Channel (Nucleus) (1 features)	X	X	√	X	√	√	√	√	√	√	√	X	X	X	√
Average of Green Channel (Nucleus) (1 features)	X	X	X	√	√	√	√	√	√	√	√	X	X	X	√
Average of Blue Channel (Nucleus) (1 features)	X	X	X	X	X	√	√	√	√	√	√	X	X	X	√
DCT (Red Channel horizontal averaged) (8 features)	X	X	X	X	X	X	√	X	√	√	√	X	√	X	√
DCT (Green Channel horizontal averaged) (8 features)	X	X	X	X	X	X	X	√	X	X	√	X	√	X	√
DCT (Blue Channel horizontal averaged) (8 features)	X	X	X	X	X	X	X	X	√	X	√	X	√	X	√
DCT block based grouping 3 channel (12 features)	X	X	X	X	X	X	X	X	X	√	X	X	X	√	√
Wavelets (Diagonal Features Red channel) (5 features)	X	X	X	X	X	X	X	X	X	X	√	√	X	X	√

These set combinations are chosen based on the classifier outcomes (by using all the features, which increase the percentage of the classifier). Also, the morphological and DCT features are combined in most of the experiment and morphological and DWT are combined in experiment 14. DCT and DWT have been combined but the result is averaged to 93%. Also, in some cases, it turns out that some features are decreasing the CA percentage but when adding another feature the CA percentage increases. The following Table presents these data:

Table 5.11 Comparison between classifier and modalities features using PC (Bolded Numbers represents the highest Classification Accuracy)


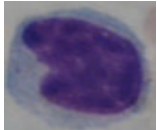
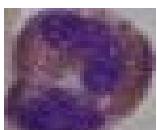
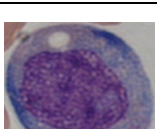
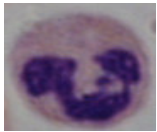
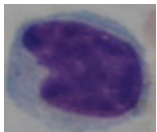
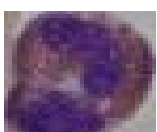
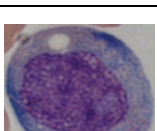
Class Name	Image related to each class	Classification Accuracy (%) of Experiment														
		1	2	3	4	5	6	7	8	9	10	11	12	13	14	15
Neutrophils (Class 1)		95.49	100.00	99.59	99.59	100.0	100.0	99.18	98.77	98.36	98.36	100.0	100.0	98.36	98.36	98.36
Lymphocytes (Class 2)		99.46	99.46	98.91	98.91	98.91	98.91	98.91	98.37	97.83	97.83	97.83	98.37	97.83	97.83	97.83
Eosinophils (Class 3)		74.19	91.94	92.74	94.35	95.97	97.58	97.58	98.39	100.0	100.0	99.19	99.19	99.19	100.0	100.0
Monocytes (Class 4)		94.51	100.0	100.0	99.39	100.0	98.78	99.39	98.78	97.56	98.17	99.39	100.0	100.0	100.0	98.17
Average		90.91	97.85	97.81	98.06	98.72	98.82	98.77	98.58	98.44	98.59	99.10	99.39	98.85	99.05	98.59

Table 5.12 Comparison between classifiers and modalities features using NN

Class Name	Image related to each class	Classification Accuracy (%) of Experiment														
		1	2	3	4	5	6	7	8	9	10	11	12	13	14	15
Neutrophils (Class 1)		72.95	77.70	95.90	91.39	82.38	74.59	99.18	72.54	87.30	96.31	94.67	92.62	89.18	75.66	98.93
Lymphocytes (Class 2)		1.99	4.89	42.02	91.85	95.11	94.57	97.83	97.28	88.59	99.46	77.83	92.93	79.02	94.02	78.37
Eosinophils (Class 3)		18.55	6.13	35.32	62.10	66.94	94.35	100.0	99.19	8.06	1.61	61.45	84.68	41.45	53.71	99.19
Monocytes (Class 4)		1.22	11.34	11.46	90.85	77.44	98.78	99.39	98.78	60.98	43.29	74.02	84.76	63.29	93.54	74.02
Average		23.68	25.02	46.18	84.05	80.47	90.57	99.10	91.95	61.23	60.17	76.99	88.75	68.24	79.23	87.63

Tables 5.11 and 5.12 show that the performance of PC second order is better compared to NN. (PC 2nd order) classifier has achieved 99.35% in 10 seconds, compared with NN which took more than in average 23 minutes with a performance of (88.75%) using the same IFV and network setup. But NN shows better results when considering experiment number seven's IFV data set. NN managed to reach 93% by combining morphological features and DCT red channel horizontal averaging method. Merging color-based morphological features with DWT or DCT features have enhanced the classification results. In NN, the CA recognition of Eosinophil is way low compared to other classes. Where in case of PC, Eosinophil CA is much better and comparable with other classes's CA. The main reason for the NN drawback in terms of classifying Eosinophil is that NN needs more features to better examine the features of the Eosinophil.

CHAPTER 6

Conclusion and Future Work

The use of an automated system to analyze blood samples is important since that it can lead to a faster classification of WBC. Also, using image processing to differentiate WBC could give various advantages including more examination accuracy, less human error and faster analysis time. Segmentation and classification of WBC could lead to appropriate analysis of human health where the ration between the types of WBC could distinguish between healthy person from a person suffering from a variety of diseases ranging from an infection to AIDS.

Segmentation of WBC from other elements in blood such as RBC, stains and platelets has proven to be a challenging exercise. In our work, adaptive thresholding based on red channel of the RGB components in conjunction with watershed algorithm, were adopted to segment WBC. Then, the WBC were allocated using computational segmentation parameters such as area, aspects ratio and color average. Also, template matching algorithm was used to allocate the WBC. Eighty percent segmentation accuracy was achieved using the adopted methodology to obtain adequate feature vector.

In this work, to classify each type of WBC, common features have to be found. This process mimics the hematologist experts who depend on area, shape, color as feature for classifying WBC in their labs. On this basis, geometrical based features, color based features, DWT based features and DCT features were extracted and analyzed. Geometrical based features resulted in adequate CA, where color based feature gives the highest CA. Combining the color morphological with some of DCT features or DWT features improved the CA.

PC gave higher classification results compared to the NN. A 99.3% CA was achieved when second order PC was used with color based morphological features in company with DWT features. Furthermore, the PC based classification was not alterative technique, since the PC classifier gave repeatable and consistent results in a very short computational time. On the other hand, NN performance was dependant on various user defined parameters network structure and randomly selected initial conditions.

The use of PC classifier in conjunction with normalization of the IFV using “Log” function enhanced the CA around 15-25% in many cases. PC has shown more tolerance to deal with the system non-linearity compared to NN. Yet, the computational time requirement, memory usage, preparation time (testing, training and averaging NN runs) is higher in NN compared with PC.

Future work can be done in improving the segmentation accuracy of the method by applying the active contour algorithm in conjunction with our method. Furthermore, there is an intension to apply the proposed algorithm on a larger WBC database.

REFERENCES

- [1] B. H. O'Connor, *A Color Atlas and Instruction Manual of Peripheral Blood Cell Morphology*, Pennsylvania: Lippincott Williams & Wilkins, 1984.
- [2] M. Sordo(msordo@dsg.bwh.harvard.edu), "Introduction to Neural Networks in Healthcare," Usenet post to <http://www.openclinical.org/neuralnetworks.html>, October 2004.
- [3] D. Anoragaingrum, "Cell Segmentation with median Filter and Mathematical morphology Operation," in *Proceedings of IEEE 10th International Conference on Image Analysis and Processing*, Vol. 9, pp. 1043, 1999.
- [4] G. Stamatoyannopoulos, P. Majerus, R. Perlmutter and H. Varmus," The Molecular Basic of Blood Diseases," W.B. Saunders Company, 3rd Edition, 2001.
- [5] W. Khiwi and M. Al-Shamsi (private communication), March 2004
- [6] S. Wick (swick@cwis.unomaha.edu),"Blood Cell Histology," Usenet post to <http://web1.tch.harvard.edu/cfapps/A2ZtopicDisplay.cfm>, June 2004.
- [7] B. Swolin and P. Simonsson, "Differential counting of blood leukocytes using automated microscopy and a decision support system based on artificial neural networks evaluation of DiffMasterTM Octavia," Vol. 25, Issue 3, pp. 139 <http://www.blackwell-synergy.com>, June 2003.
- [8] N. Mead, "A New Vision of Research," Usenet post to <http://www.whitaker.org/abstracts/rgmay96.html>, November 2004.
- [9] H. Hengen, O. Gabel, A. Hajra, T. Paulus, M. Ross and S. Spoor, "Development of a system for the analysis and classification of blood and bone marrow cell images to support morphological diagnosis of leukemia," Kaiserslautern, Germany, February 2004. <http://www.eit.uni-kl.de/pandit/main/forschung/blutzellene.htm>
- [10] D. M. U. Sabino, L. da F. Costa, E. G. Rizzatti and M. A. Zago, "A texture approach to leukocyte recognition," *Real-Time Imaging*, Vol.10, pp. 205–216, Usenet post to <http://www.cse.iitd.ernet.in/~csa03027>, February 2004.

- [11] Q. Zheng, B. K. Milthorpe, and A. Jones, "Direct Neural Network Application for Automated Cell Recognition," 2003, Wiley-liss, Inc, Cytometry Part A, Vol. 57A, pp 1-9, 2004.
- [12] L. Yang, P. Meer and D. J. Foran, "Unsupervised Segmentation Based on Robust Estimation and Color Active Contour Models," IEEE, Usenet post to <http://www.caip.rutgers.edu/riul/research/papers/pdf/snake.pdf>, January 2004.
- [13] N. Sinha (neelam@ee.iisc.ernet.in) and A. G. Ramakrishnan (ramkiag@ee.iisc.ernet.in), "Automation of Differential Blood Count," Bio-Medical Lab, Department of Electrical Engineering, Indian Institute of Science, Bangalore, IEEE, 2003.
- [14] G. Ongun, U. Halici, K. Leblebicioglu and V. Atalay, "Feature Extraction and Classification of Blood Cells for an Automated Differential Blood Count System," *IEEE International Joint Conference on Neural Networks*, pp. 2461-2466, 2001.
- [15] S. F. Bikhet and A. M. Darwish and H. A. Tolba and S. I. Shaheen, "Segmentation and Classification of White Blood Cells," *IEEE International Conference On Acoustics, Speech and Signal Processing, ICASSP*, pp. 2259-2261, 1999.
- [16] J. Park and J. Keller, "Fuzzy Patch Label Relaxation in Bone Marrow Cell Segmentation," *A Computational Intelligence System for Cell Classification*, pp. 1133-1138, 1997.
- [17] R. Gonzalez and R. Woods, *Digital Image Processing*, New Jersey: Prentice-Hall, 2002.
- [18] J. Russ, *The Image Processing Handbook*, New York: CRC press, 2002.
- [19] W. B. Penne baker and J. L. Mitchell, "JPEG: Still Image Data Compression Standard," Massachusetts: Kluwer Academic Publishers, 1992.
- [20] N. Otsu, "A thresholding selection method from gray-level histogram," *IEEE Transactions on Systems, Man, and Cybernetics*, Vol. 8, pp. 62-66, 1978.
- [21] S. Beucher, Watershed, hierarchical segmentation and waterfall algorithm. In *Mathematical Morphology and its Applications to Image Processing*, J. Serra and P. Soille, Eds. Kluwer Academy Publishers, Dordrecht, pp. 69-76, 1994.

- [22] J. Park and J. M. Keller, "Snakes on the Watershed," *IEEE Transactions on pattern analysis and machine intelligence*, Vol. 23, No.10, pp. 1201-1205, October 2001.
- [23] H. Hengen (Heiko.Hengen@eit.uni-kl.de), S. Spoor (Susanne.Spoor@eit.uni-kl.de) and Pandit M., Electrical Engineering and Information Technology, University of Kaiserslautern in Germany, "Analysis of Blood and Bone Marrow Smears using Digital Image Processing Techniques", 2002. Usenet post to <http://www.eit.uni-kl.de/pandit/main/forschung/blutzellene.htm>, June 2004.
- [24] T. Wittman, "Face Detection in Crowded Images," Department of Mathematics, University of Minnesota. Usenet post to <http://www.math.umn.edu/~wittman/faces/main.html>, June 2004.
- [25] J. A. Richards, *Remote Sensing Digital Image Analysis*, Berlin: Springer-Verlag, 1993.
- [26] C. S. Burrus, R. A. Gopinath, and H. Guo, *Introduction to wavelets and Wavelet Transform*, New Jersey: Prentice-hall International, Inc., 1998.
- [27] R. K. Young, *Wavelets Theory and its Applications*, Boston: Kluwer Academic Publishers, 1993.
- [28] S. Mallat, "A Theory of Multiresolution Signal Decomposition: The Wavelet Representation," *IEEE Transaction Pattern Analysis and Machine Intelligence*, vol. 11, pp. 674-693, 1989.
- [29] K. R. Rao, *Discrete Cosine Transform: Algorithms, Advantages, Applications*, San Diego: Academic Press Professional Inc., 1990.
- [30] E. M. Petriu (petriu@site.uottawa.ca), "Neural Networks :Basics", School of Information Technology and Engineering, University of Ottawa, Canada, Usenet post to <http://www.site.uottawa.ca/~petriu/>, November 2004.
- [31] T. Reil (torsten.reil@zoo.ox.ac.uk), "Artificial Neural Networks," Usenet post to <http://www.zoo.ox.ac.uk/>, November 2004

[32] W. Campbell, K. Assaleh and C. Broun, "Speaker recognition with polynomial classifiers," *IEEE Transactions on Speech and Audio Processing*, Vol.10, No. 4, pp. 205-212, 2002.

[33] V. Wan and S. Renals, "Evaluation of Kernel Methods for Speaker Verification and Identification," In *Proc IEEE International Conference on Acoustics, Speech, and Signal Processing*, vol. 1, pp. 669-672, 2002,
<http://www.cstr.ed.ac.uk/downloads/publications/2002/thesis.pdf>.

[34] W. M. Campbell and K. T. Assaleh, "Polynomial classifier techniques for speaker verification," in *Proc. IEEE International Conference on Acoustics, Speech, and Signal Processing*, vol. 1, pp. 321-324, 1999.

VITA

Juma A. Bin Darwish Al-Muhairy was born on June 19, 1979, in Dubai, United Arab Emirates. He was educated in local public schools and graduated from Al-Waheida High School in 1997. He receives a scholarship from Abu Dhabi Authority of Investments to Northeastern University in Boston, Massachusetts, United States of America, from which he graduated cum laud, in 2001. His degree was a Bachelor of Science in Electrical Engineering with a concentration in Computer Engineering.

Mr. Al-Muhairy moved to the United Arab Emirates in 2001 and worked as an AV and Security Engineer for three years at Department of Civil Aviation in Dubai, UAE. In 2002, Mr. Al-Muhairy began a master's program in Mechatronics at the American University of Sharjah. In 2004, Mr. Al-Muhairy moved to work as Manager - Electrical and Electronic Systems up to date at the Dubai World Trade Center. He was awarded with the Master of Science degree in Mechatronics in 2005.

Mr. Al-Muhairy is a member of IEEE.